*Economic Geology,* v. 100, pp. 863–886

# Bajo de la Alumbrera Copper-Gold Deposit: Stable Isotope Evidence for a Porphyry-Related Hydrothermal System Dominated by Magmatic Aqueous Fluids

ANTHONY C. HARRIS,[†,*] SUZANNE D. GOLDING, AND NOEL C. WHITE

*Department of Earth Sciences, University of Queensland, 4072 Brisbane, Australia*

## Abstract

Alteration zones at the gold-rich Bajo de la Alumbrera porphyry copper deposit in northwestern Argentina are centered on several porphyritic intrusions. They are zoned from a central copper-iron sulfide and gold-mineralized potassic (biotite-K-feldspar ± quartz) core outward to propylitic (chlorite-illite-epidote-calcite) assemblages. A mineralized intermediate argillic alteration assemblage (chlorite-illite ± pyrite) has overprinted the potassic alteration zone across the top and sides of the deposit and is itself zoned outward into phyllic (quartz-muscovite-illite ± pyrite) alteration. This study contributes new data to previously reported $\delta^{18}O$ and $\delta D$ compositions of fluids responsible for the alteration at Bajo de la Alumbrera, and the data are used to infer likely ore-forming processes.

Measured and calculated $\delta^{18}O$ and $\delta D$ values of fluids (+8.3 to +10.2 and –33 to –81‰, respectively) confirm a primary magmatic origin for the earliest potassic alteration phase. Lower temperature potassic alteration formed from magmatic fluids with lower $\delta D$ values (down to –123‰). These depleted compositions are distinct from meteoric water and consistent with degassing and volatile exsolution of magmatic fluids derived from an underlying magma. Variability in the calculated composition of fluid associated with potassic alteration is explained in terms of phase separation (or boiling). If copper-iron sulfide deposition occurred during cooling (as proposed elsewhere), this cooling was largely a result of phase separation.

Magmatic water was directly involved in the formation of overprinting intermediate argillic alteration assemblages at Bajo de la Alumbrera. Calculated $\delta^{18}O$ and $\delta D$ values of fluids associated with this alteration range from +4.8 to +8.1 and –31 to –71 per mil, respectively. Compositions determined for fluids associated with phyllic alteration (–0.8 to +10.2 and –31 to –119‰) overlap with the values determined for the intermediate argillic alteration. We infer that phyllic alteration assemblages developed during two stages; the first was a high-temperature (400°–300°C) stage with D-depleted water ($\delta D$ = –66 to –119‰). This compositional range may have resulted from magma degassing and/or the injection of new magmatic water into a compositionally evolved hydrothermal system. The isotopic variations also can be explained by increased fluid-rock interaction. The second stage of phyllic alteration occurred at a lower temperature (~200°C), and variations in the modeled isotopic compositions imply mixing of magmatic and meteoric waters. Ore deposition that occurred late in the evolution of the hydrothermal system was probably associated with further cooling of the magmatic fluid, in part caused by fluid-rock interaction and phase separation. Changing pH and/or oxygen fugacity may have caused additional ore deposition. The ingress of meteoric water appears to postdate the bulk of mineralization and occurred as the system at Bajo de la Alumbrera waned.

## Introduction

METEORIC WATER has long been thought to play a major role in hydrothermal alteration and ore deposition processes in porphyry ore deposits (e.g., Sheppard et al., 1969) and has been envisaged as an integral part of the huge hydrothermal systems developed in and around mineralized porphyritic intrusions in the shallow crust (e.g., Gustafason and Hunt, 1975). The importance of magmatic fluids is well established, with magma degassing and volatile exsolution causing plumes of metal- and volatile-rich magmatic aqueous fluids to be released (Hedenquist and Lowenstern, 1994, and references therein). These magmatic fluids cause the earliest hydrothermal alteration and are thought to be responsible for the bulk of mineralization in most porphyry copper deposits (e.g., Meyer and Hemley, 1967; Lowell and Guilbert, 1970; Beane and Titley, 1981). Mixing of meteoric water into the magmatic fluids was thought to explain the concentrically arranged alteration zones seen in porphyry copper deposits (Lowell and Guilbert, 1970; DeGeoffroy and Wignall, 1972). Some studies also used this mixing to explain the source of the vast quantities of metals and fluids needed to form these deposits (Hall et al., 1974; Batchelder, 1977).

Numerous detailed fluid inclusion studies have found high-temperature (in excess of 450°C) vapor and coexisting hypersaline liquid inclusions (up to 70 wt % NaCl equiv) in potassic alteration assemblages (e.g., Roedder, 1971; Moore and Nash, 1974; Gustafson and Hunt, 1975; Eastoe, 1978; Ahmad and Rose, 1980; Beane and Titley, 1981). Furthermore, fluid inclusion studies found that lower temperature (<350°C) and less saline (<5 wt % NaCl equiv) liquid inclusions dominate in the late stage (and commonly peripheral) phyllic alteration zone. The accepted genetic model (e.g., Lowell and Guilbert, 1970; Beane and Titley, 1981; Reynolds and Beane, 1985) explained this temporal variation by the mixing of meteoric water into the magmatic fluid. Support for this model comes from $\delta^{18}O$ and $\delta D$ values of hydrothermal minerals (e.g., Sheppard et al., 1969, 1971; Taylor, 1974; Sheppard and Gustafson, 1976).

With its concentric zonal arrangement of hydrothermally altered rocks, the Bajo de la Alumbrera porphyry copper-gold deposit, northwestern Argentina is a classic example of a porphyry ore deposit and observations made there have played a

[†] Corresponding author: e-mail, A.Harris@utas.edu.au

[*] Present Address: Centre of Excellence in Ore Deposits, Private Bag 79, University of Tasmania, 7001, Hobart, Australia.

significant role in the accepted descriptive and genetic models of porphyry copper deposits (e.g., Sillitoe, 1973). At Bajo de la Alumbrera, the magmatic hydrothermal system developed in and around multiple intrusions (Proffett, 2003). Miarolitic cavities and other key textures found in these intrusions imply that some magma batches ascended with potentially metal-rich magmatic fluids (Harris et al., 2004a). Extremely copper rich fluid inclusions coexist with composite melt-fluid inclusions in the earliest magmatic hydrothermal quartz veins (Harris et al., 2003), which together with petrographic observations of primary igneous textures, link volatile exsolution of the magma with ore-bearing hydrothermal alteration. Detailed fluid inclusion studies using laser ablation inductively coupled plasma-mass spectrometry (ICP-MS) analysis, combined with stable isotope analyses, have helped to constrain the chemical and physical evolution of the ore fluids at Bajo de la Alumbrera (Ulrich et al., 2002). The current study has extended this work in order to evaluate the relative importance of magmatic and meteoric fluids to the development of hydrothermal alteration assemblages in the Bajo de la Alumbrera deposit. New stable isotope analyses and fluid inclusion microthermometry of alteration assemblages are used to assess the abundance of magmatic hydrothermal fluids in the various paragenetic stages and to infer likely ore-forming processes.

## Geology of the Bajo de la Alumbrera Deposit

Bajo de la Alumbrera is a late Miocene gold-rich porphyry copper deposit. It contains 402 million metric tons (Mt) at 0.54 percent copper and 0.64 g/t gold (Proffett, 2003). Numerous published and company reports document the intrusions, hydrothermal alteration, and deposit paragenesis (e.g., González, 1975; Godeas and Segal de Svetliza, 1980; Stults, 1985; Dawson, 1994; Guilbert, 1995; Méndez, 1997). Crosscutting relationships of intrusions and relative timing of hydrothermal alteration assemblages have been documented by Proffett (J.M. Proffett, unpub. report for Minera Alumbrera Ltd., 85 p., 1995; J.M. Proffett, unpub. report for Minera Alumbrera Ltd., 169 p., 1997; Proffet, 2003). Ulrich (1999), Ulrich and Heinrich (2002), and Ulrich et al. (2002) were the first to attempt to unravel the fluid evolution of the porphyry system at Bajo de la Alumbrera, based on detailed microanalysis of fluid inclusions and stable isotope geochemistry. They documented the deposit-scale distribution of different fluid inclusion types and related this to the broad zonation of hydrothermal alteration assemblages at Bajo de la Alumbrera.

Mineralization and hydrothermal alteration at Bajo de la Alumbrera occurred within and around several high K calc-alkaline to shoshonitic plagioclase-biotite (hornblende)-phyric dacitic porphyries (Proffett, 1997, writ. commun.; 2001, 2003; Sasso and Clark, 1998; Ulrich and Heinrich, 2002; Harris et al., 2004a). The porphyries intruded a low-standing multiple-vent volcanic complex, which developed in an intermontane sedimentary basin (Clark et al., 1976; Caelles et al., 1971; Figueroa, 1971; Llambías, 1972; Sasso and Clark, 1998; Harris et al., 2004b). A linear deformation zone marking the boundary between two major physiotectonic terranes (Puna-Altiplano and the Sierras Pampeanas) confined the basin (Fig. 1; de Urreiztieta et al., 1996). Volcanism in the area surrounding Bajo de la Alumbrera (Fig. 2) began at about 8.5 Ma

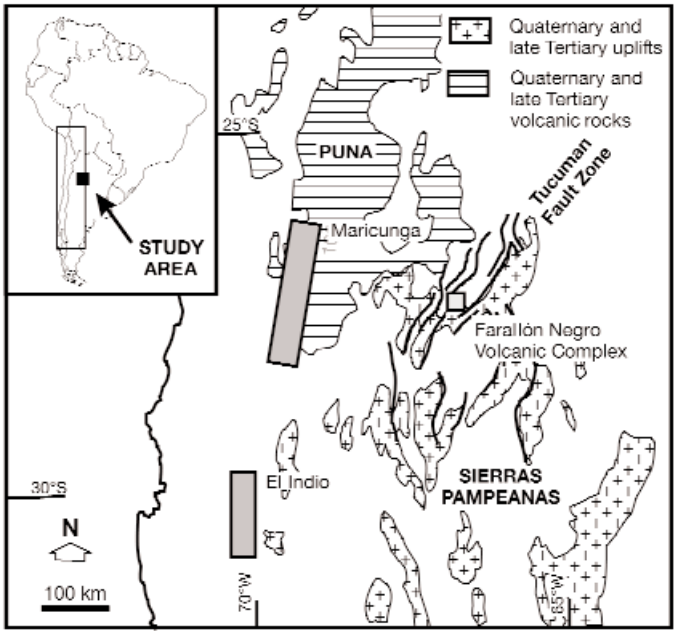


FIG. 1. Map of the central Andes, showing the location of the Farallón Negro Volcanic Complex, in which the Bajo de la Alumbrera porphyry copper-gold deposit occurs. The Farallón Negro district is an intermontane basin within a structural deformation zone referred to as the Tucuman fault zone. The fault zone marks the transition between the Puna-Altiplano to the north and the Sierras Pampeanas to the south (modified after Ulrich and Heinrich, 2002; Proffett, 2004). Important Neogene mineralized districts are also shown by the gray boxes, including the Maricunga and El Indio districts (modified after Kay et al., 1999).

(more regionally at 12.5 Ma; Harris et al., 2004, and references therein), synchronous with uplift of the crystalline basement of the Sierras Pampeanas terrane (Jordan and Allmendinger, 1986; Reynolds et al., 1987; Strecker et al., 1989, Tabbutt, 1990; Coughlin et al., 1998).

### *Intrusion characteristics*

Despite uncertain field relationships (Proffett, writ. commun., 2001; Ulrich and Heinrich, 2002), the oldest porphyry intrusion is thought to be the NE Porphyry. Where seen, the NE Porphyry is cut by all hydrothermal alteration stages (J.M Proffett, writ. commun., 2003). Another early intrusion, referred to as the Los Amarillos Porphyry, is a fragmented biotite-plagioclase-phyric dacite in which destructive alteration assemblages have obscured the primary igneous textures. Field relationships combined with U-Pb geochronology suggest that this porphyry predated all main-stage mineralized intrusions (Fig. 3; Proffett, 2003; Harris et al., 2004b).

The P2 Porphyry is the earliest mineralized porphyry (Fig. 4; Proffett, 2003). It is pervasively altered to potassic mineral assemblages. Based on relict phenocrysts, the P2 is a plagioclase (biotite-hornblende)-phyric dacite. As P2 lacks quartz vein fragments and does not truncate quartz veins, Proffett (2003) attributed the bulk of the mineralization at Bajo de la Alumbrera to this porphyry.

The Early P3 Porphyry is a biotite-bearing plagioclase-phyric dacite that contains fragments of andesite wall rock and mineralized quartz veins. Different intrusive phases are discriminated on the basis of macrocryst type (Proffett, 2003).

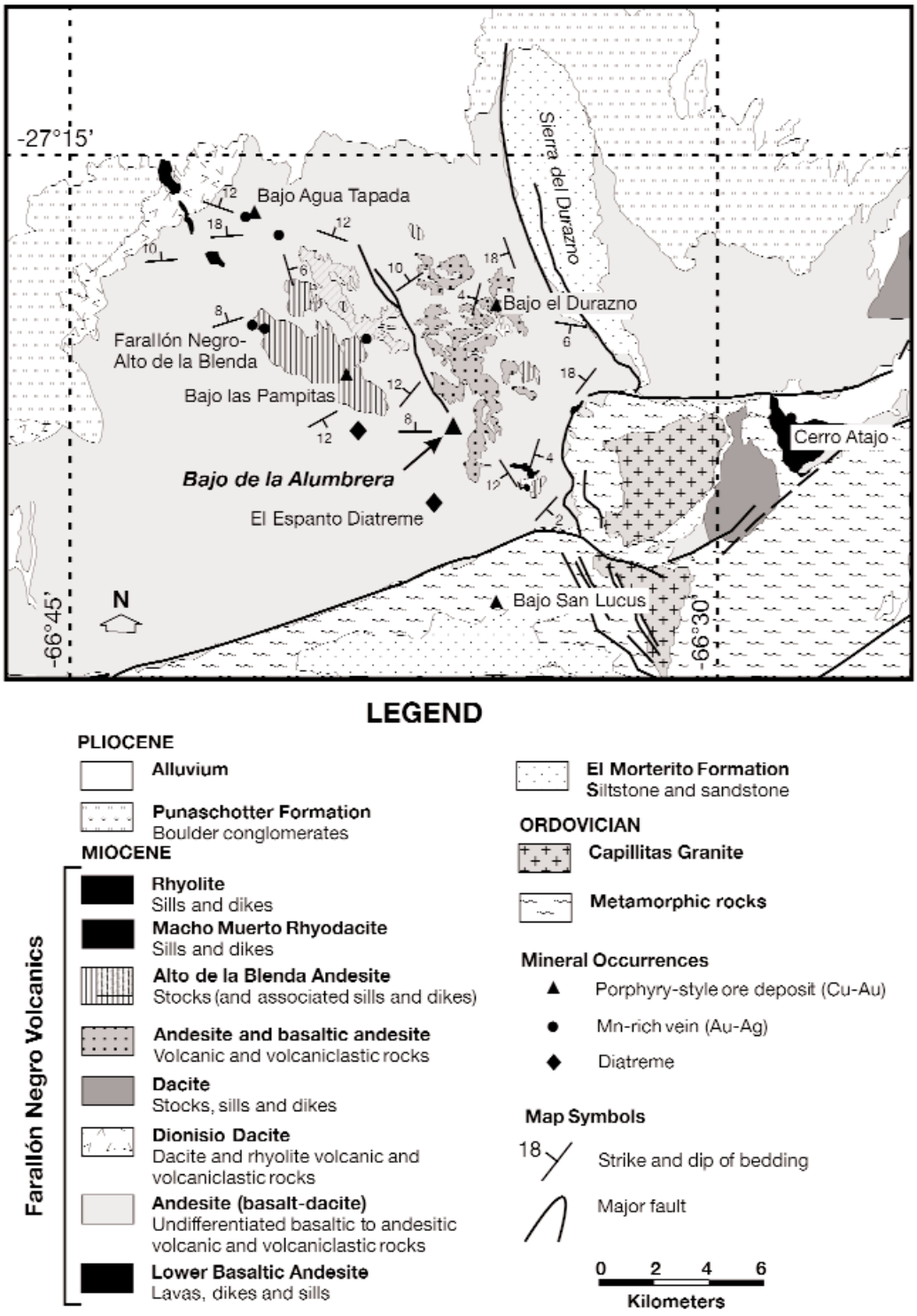


FIG. 2. Geologic map of the Farallón Negro Volcanic Complex (modified after Proffett, 1997, 2003; Sasso, 1997; reproduced from Harris et al., 2004a).

The Quartz Eye Porphyry is distinguished from the Early P3 Porphyry by abundant quartz phenocrysts. The Late P3 porphyries, including the North and Campamento porphyries as defined by Proffett (2003), are a group of hornblende-bearing plagioclase-phyric dacite porphyries that contain distinctive euhedral biotite books. At depth, some of these intrusive phases change texturally, becoming more equigranular and coarser grained as well as monzonitic in composition. Although they are altered to potassic and propylitic assemblages and are weakly veined by quartz, the Late P3 porphyries were intruded later than main-stage mineralization (Proffett, writ. commun., 2001, 2003; Ulrich and Heinrich, 2002). The Late

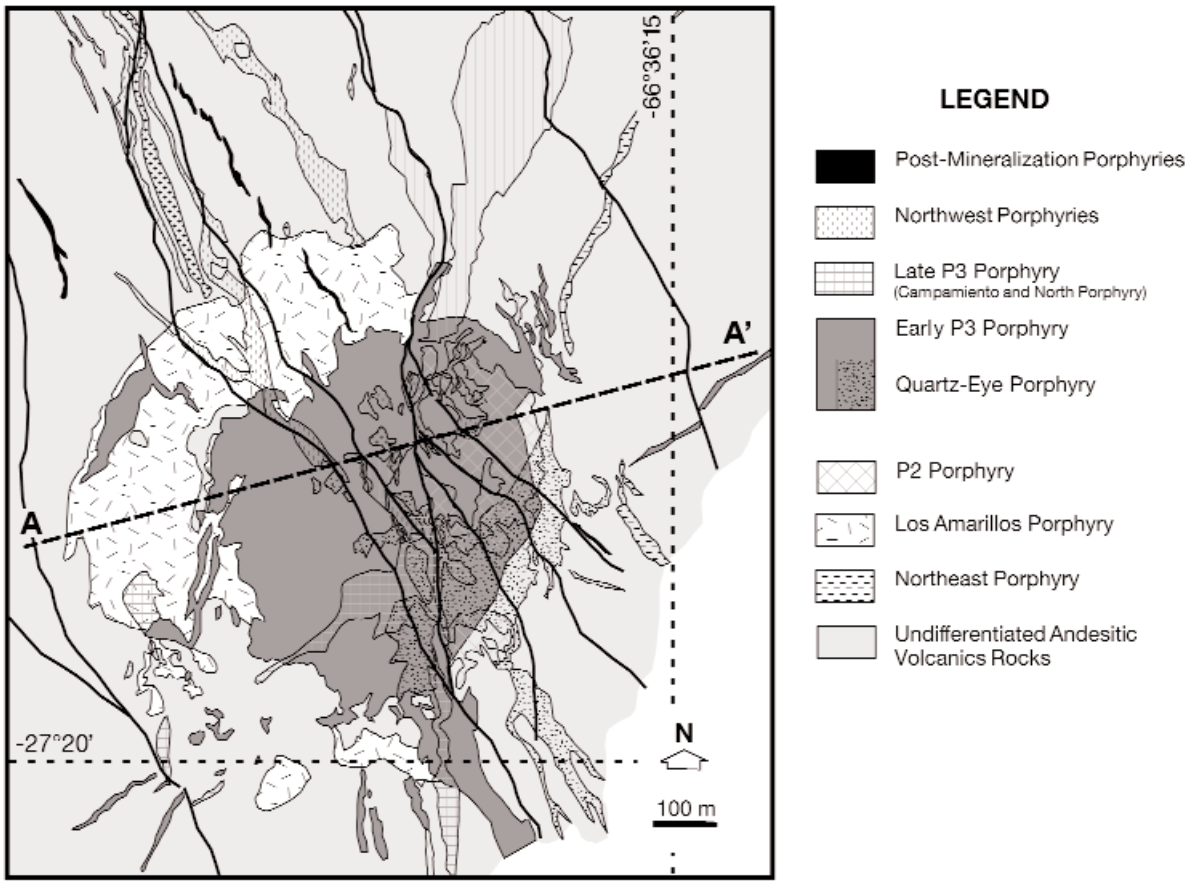


FIG. 3. Geologic map of intrusive rocks in the Bajo de la Alumbrera deposit (modified after Proffett, 2003). Faults mapped by Proffett (2003) are marked as solid black lines.

P3 porphyries have low copper and gold contents and have intruded rocks that are well mineralized.

U-Pb zircon ages show that at least two phases of biotite-phyric dacite porphyry emplacement occurred at Bajo de la Alumbrera (Harris et al., 2004b), namely an 8.0 Ma event that includes the Los Amarillos and P2 porphyries (8.02 ± 0.14 and 7.98 ± 0.14 Ma) and a 7.0 Ma event that includes the P3 porphyries (7.10 ± 0.07 Ma; Fig. 4). Dating of unaltered subvolcanic intrusions from the surrounding district reveals that where known the zircon U-Pb ages are within analytical uncertainty of hornblende $^{40}Ar/^{39}Ar$ ages (Sasso, 1997; Sasso and Clark, 1998; Harris et al., 2004b). As such it appears that the zircon U-Pb ages are indistinguishable from the time at which single intrusions cooled through 500°C (or the Ar-based blocking temperature of hornblende). Based on this finding, the U-Pb ages approximate the timing of porphyry emplacement at Bajo de la Alumbrera (cf. Halter et al., 2004a).

The available geochronologic data also show that regional magmatism persisted for a little more than 2.0 m.y. (Halter et al., 2004a, b). These constraints combined with crosscutting relationships indicate that basaltic andesite and andesite intrusions were contemporaneous with the more silicic dacite porphyries at Bajo de la Alumbrera (Harris et al., 2004b). Petrographic and geochemical evidence shows that mingling and/or incomplete mixing was important in the petrogenesis of the Farallón Negro Volcanics (Sasso, 1997; Harris, 2002; Ulrich and Heinrich, 2002; Halter et al., 2004b). The occurrence of mafic inclusions, sieve textures, and the presence of internal resorption discontinuities in plagioclase (Sasso, 1997) are, in part, evidence for magma mixing and/or mingling (e.g., Pallister et al., 1996). These observations have been corroborated by geochemical data (Halter et al., 2004b).

*Alteration and vein paragenesis*

The paragenetic sequence of Bajo de la Alumbrera reported here is a simplification of the framework established by Proffett (J.M. Proffett, unpub. report for Minera Alumbrera Ltd., 169 p., 1997; Proffet, 2003) and that published by Ulrich and Heinrich (2002; Fig. 4). Alteration has produced a concentrically zoned pattern from a central potassic (K-feldspar-biotite ± quartz ± magnetite) core, out to distal propylitic (chlorite-illite-epidote-calcite) assemblages (Fig. 5, Table 1; see also Stults, 1985; Guilbert, 1995). An intermediate argillic (chlorite-illite ± pyrite) alteration assemblage overprinted part of the potassic zone and appears, in part, to be synchronous with the phyllic alteration assemblage. The phyllic (quartz-muscovite-illite ± pyrite) alteration assemblages rim the potassic alteration zone and extend downward along its edges (Fig. 5; Proffett, 2003). In addition, we have found crosscutting vein relationships that indicate multiple stages of phyllic and intermediate argillic alteration. Carbonate-base

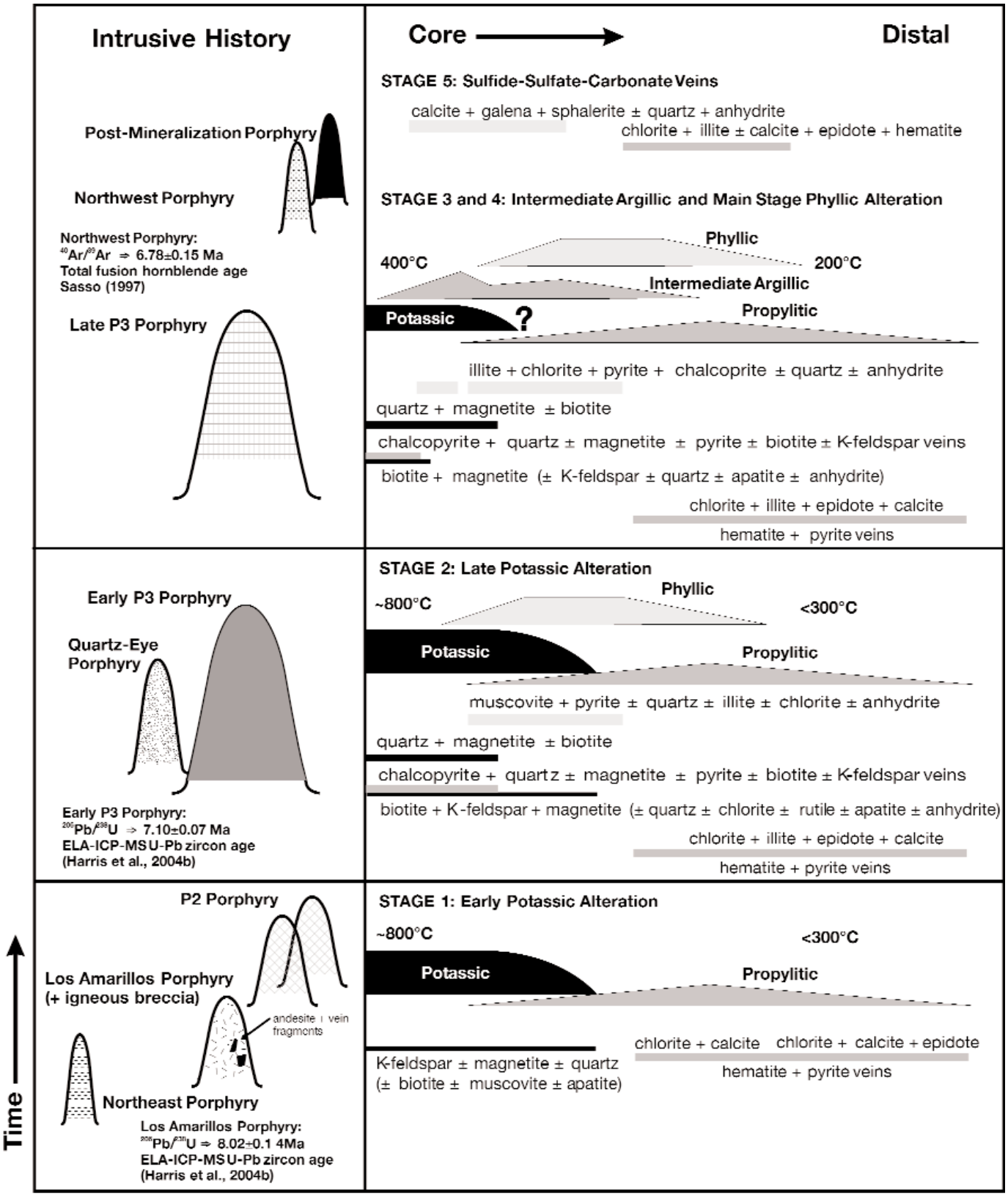


FIG. 4. Generalized time (vertical) vs. space (distance and depth) diagram, showing the sequence of events leading to the current configuration of alteration assemblages at Bajo de la Alumbrera (modified after Ulrich and Heinrich, 2002; Proffett, 2003).

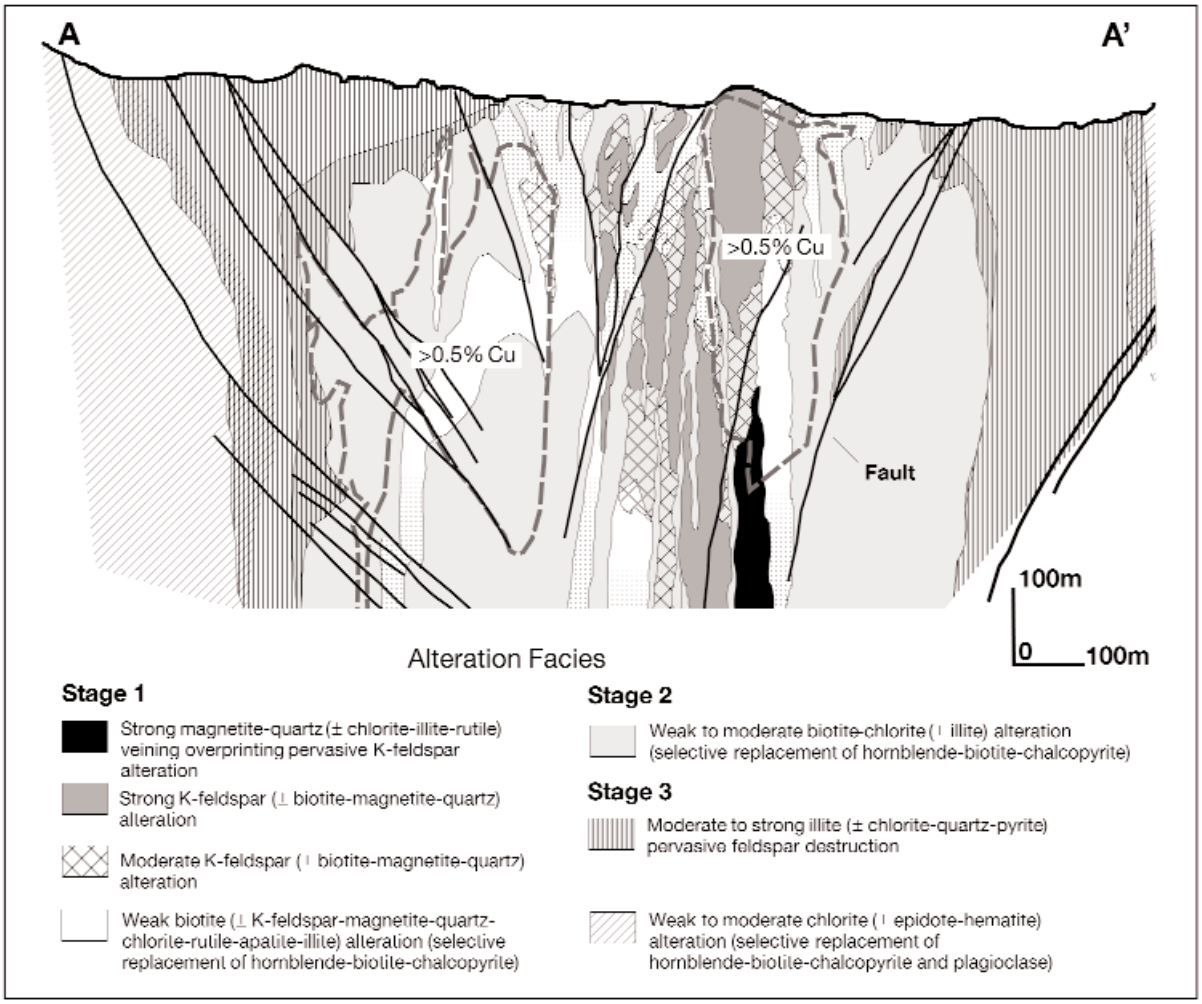


FIG. 5. Cross section through the Bajo de la Alumbrera porphyry-related hydrothermal system, showing the zonal distribution of alteration minerals. Location (A-A') shown in Figure 3. Modified after Proffett (2003) and used with permission from J.M. Proffett (2001).

metal assemblages occur as fault and fracture fill and are interpreted to have formed during the final phase of hydrothermal activity.

Potassic alteration produced an early-formed K-feldspar-magnetite-quartz ± biotite assemblage (stage 1) and a later biotite-magnetite-quartz ± K-feldspar assemblage (stage 2; Table 1). Diffuse veins, similar to the "A veins" defined by Gustafson and Hunt (1975), were synchronous with and have locally cut the K-feldspar alteration assemblages (Fig. 6A). They have equigranular quartz (and lesser amounts of K-feldspar ± hornblende ± biotite ± magnetite) with chalcopyrite and lesser amounts of pyrite; these are the P veins of Harris et al. (2003). Thick, irregular veins of rose quartz-chlorite ± chalcopyrite ± pyrite ± anhydrite are either associated with the K-feldspar alteration or predate the bulk of the potassic alteration (J.M. Proffett, pers. commun., 2003). Quartz typically occurs as coarse-grained hexagonal crystals (<8 mm). Crustiform textures are characteristic, with fine-grained vein margins and coarse-grained cores. These veins are vuggy in the uppermost levels of the deposit.

Magnetite-quartz and quartz-only veins occur as a dense irregular stockwork in the deposit core (Ulrich and Heinrich, 2002; Proffett, 2003). Chalcopyrite occurs sporadically throughout the upper parts of this vein network. Quartz and magnetite are typically banded within individual veins. Intergrowths of K-feldspar and hornblende are common. In some areas, primary rock textures have been obliterated and the rock is composed entirely of massive, sugary magnetite and quartz. Magnetite veinlets and quartz-magnetite veins have a sparse distribution away from the core but still can be recognized at the periphery of the deposit. They are more abundant in the Early P3 Porphyry than in the adjacent andesite wall rocks.

The biotite alteration assemblage comprises pervasive biotite, K-feldspar, and magnetite and has, in part, overprinted the earliest potassic assemblages (Fig. 6B, C). Sulfide mineralization in this alteration stage is more intensely developed in the andesite, with chalcopyrite and pyrite occurring in quartz microveinlets. By contrast, chalcopyrite is commonly disseminated in the porphyritic rocks. Irregular stockworks

TABLE 1. Summary of Alteration Stages and Their Distribution at Bajo de la Alumbrera[1]

| Alteration stage | Alteration term | Description | Mineralization | Alteration distribution |
|---|---|---|---|---|
| Stage 1 | Potassic (K-feldspar-rich) | Pervasive K-feldspar-magnetite-quartz ± biotite-muscovite-apatite with disseminated chalcopyrite-bornite; veins and veinlets of quartz-magnetite, quartz-chlorite ± chalcopyrite-pyrite; mosaic intergrowth of K-feldspar-quartz ± magnetite replaces phenocrysts in porphyries; elsewhere, this assemblage comprises clots of K-feldspar surrounded by a corona of fine K-feldspar-muscovite-quartz-apatite and phenocrysts of biotite that have been partly replaced by K-feldspar-muscovite ± magnetite | Copper-iron sulfides are uncommon in this alteration phase, occurring typically in the upper portions of the deposit; chalcopyrite dominates with lesser bornite | K-feldspar–rich assemblage alters the P2 Porphyry where pervasive K-feldspar replacement of groundmass and phenocrystic feldspars has occurred |
| Stage 1 (periphery) | Propylitic | Clots of chlorite-illite ± carbonate-epidote-hematite and carbonate rimmed by chlorite; pervasive alteration of andesite; veinlets of illite-chlorite crosscut the pervasive alteration; in the peripheral zone, magnetite-biotite-quartz veins occur and are interpreted to be related to the potassic alteration assemblages | Copper-iron sulfides are uncommon, with pyrite most abundant | Outermost alteration zone that surrounds the central potassic core |
| Stage 2 | Potassic (biotite-rich) | Pervasive biotite-K-feldspar-magnetite ± quartz-chlorite-rutile-apatite; disseminated chalcopyrite and veinlets of chalcopyrite-pyrite-quartz; phenocrystic biotite is recrystallized with groundmass feldspars altered to a mosaic of K-feldspar ± biotite-quartz-chlorite-rutile-apatite; magnetite occurs as disseminations intergrown with shredded biotite; andesitic volcanic rocks are intensely altered to very fine grained biotite intergrown with K-feldspar and magnetite; stockworks of chalcopyrite-quartz ± magnetite-pyrite-biotite-K-feldspar ("B veins") are cut by quartz-molybdenite ± anhydrite | Bulk of the copper-iron sulfides (and by inference gold) believed to be associated with this alteration zone | Commonly overprints the pervasive K-feldspar alteration; most abundant in the andesite volcanic rocks |
| Stage 3 (central zone) | Intermediate argillic | Pervasive chlorite-illite ± rutile-magnetite-pyrite-chalcopyrite alteration overprinted by chalcopyrite-quartz-anhydrite-chlorite ± illite veins, illite-pyrite-quartz ± anhydrite veins and by late pyrite-calcite-chlorite ± quartz-anhydrite veins | Possibly associated with significant copper-gold grade, however, this zone overprints the earlier potassic zones | Typically overprints the pervasive biotite alteration |
| Stage 4 | Phyllic | Characterized by zones of muscovite-illite ± carbonate-chlorite-pyrite-chalcopyrite; clots of muscovite (phengite)-chlorite ± carbonate-hematite-illite occur in the deepest portions of the deposit and the transitional zone into the central potassic alteration; discontinuous trails and veins of illite-quartz-anhydrite ± pyrite-chalcopyrite ("D veins") and late pyrite-calcite-chlorite ± quartz-anhydrite cut the pervasive phyllic alteration; late pyrite-calcite-chlorite ± quartz-anhydrite veins cut the illite-quartz-anhydrite veins of the periphery of the deposit | Visible copper-iron sulfide mineralization, but timing is uncertain because of overprinting | Occurs across the top of the deposit and on the periphery of the potassic alteration zone, extending to the base of economic mineralization; muscovite-dominated assemblages occur in the deepest portions of the deposit and grade upward to illite-dominated phyllic alteration |
| Stage 5 | Pb-Zn sulfide, sulfate-carbonate veins | Carbonate (calcite-dolomite-ankerite)-galena-sphalerite ± quartz-anhydrite-montmorillonite-nontronite veins | Lead-zinc sulfides | Overprints the central potassic and intermediate argillic alteration core; sulfides have a late timing, possibly linked to the final stages of phyllic alteration |

Alteration mineralogy determined using petrographic observations combined with XRD analyses and use of a portable short wave length infrared field spectrometer

[1] Compilation of data from J.M. Proffett (writ. commun., 2001, 2003), Ulrich and Heinrich (2002), and this study

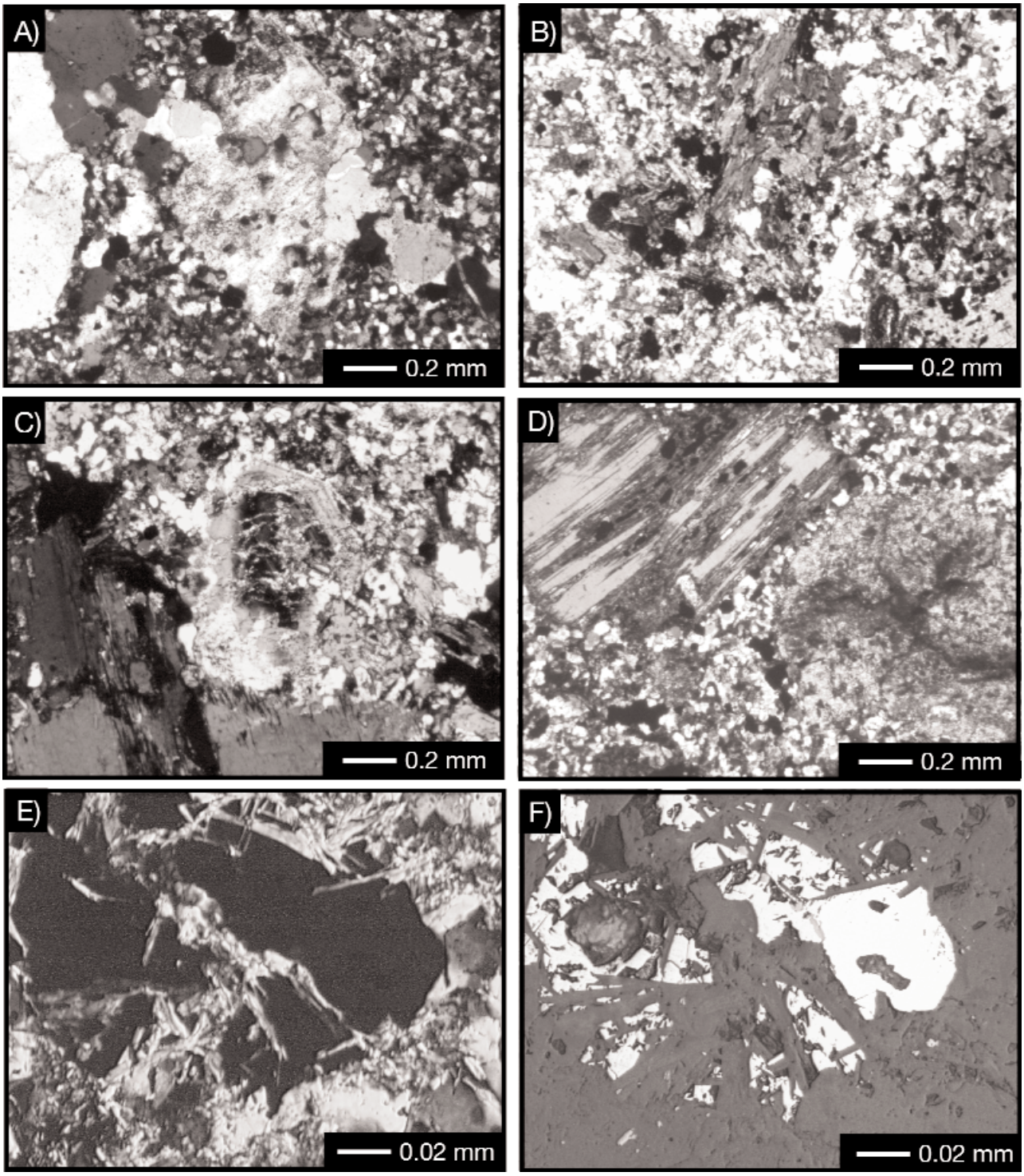


FIG. 6. Photomicrographs of hydrothermal alteration assemblages from Bajo de la Alumbrera. A. Irregular quartz vein trending from the top left-hand corner to the bottom right. Note the coarse mosaic of K-feldspar altered groundmass (stage 1). B. A clot of ragged secondary biotite surrounded by fine-grained secondary K-feldspar has replaced groundmass feldspars (stage 2). C. Secondary biotite, which has enclosed a partly illite altered plagioclase crystal. D. Partial replacement of a biotite phenocryst by chlorite-magnetite. The feldspar on the right hand side of the photomicrograph has been replaced by illite. Note that this selective intermediate argillic alteration (stage 3) has overprinted K-feldspar-(or stage 1 potassic-) altered primary groundmass feldspars. E. Pyrite and chalcopyrite (black, opaque minerals) are intergrown with coarse, euhedral blades of illite (stage 4) and anhedral quartz (transmitted light). F. Reflected light photomicrograph of (E). Note that a thin quartz-magnetite vein cuts this assemblage.

of chalcopyrite-quartz ± magnetite ± pyrite ± biotite and K-feldspar have overprinted the biotite alteration zone (stage 2). These veins contain most of the copper and gold. They are 1 to 10 mm wide, irregular to curviplanar veins that have subhedral quartz crystals along their margins and a continuous central seam of chalcopyrite. Although no gold was observed in this study, it is known to occur as small grains at the margins of chalcopyrite crystals (Dawson, 1994; Ulrich, 1999). Additionally, small gold grains occur adjacent to magnetite, pyrite, and K-feldspar (Dawson, 1994).

Propylitic alteration assemblages probably formed coevally with and peripheral to the potassic zone (Proffett, 2003). Typically, the propylitic zone comprises clots of chlorite-illite ± carbonate-epidote and magnetite (in part, altered to hematite) that have pervasively altered the groundmass feldspars and ferromagnesian minerals of the andesitic volcanic rocks. Clots of carbonate rimmed by chlorite commonly replaced coarser phenocrystic plagioclase. Veinlets of illite and some chlorite cut the pervasively altered rocks.

Mineral assemblages similar to the propylitic assemblage (chlorite-illite ± rutile ± magnetite) have overprinted the inner potassic zone (stage 3; Table 1). Based on the mineralogy, this zone is referred to as intermediate argillic alteration (or SCC, as defined by Sillitoe and Gappe, 1984, and summarized by Sillitoe, 2000). The intermediate argillic alteration zone appears to grade outward to phyllic alteration and overprints, in part, both the K-feldspar and biotite alteration assemblages (Fig. 7). It is most strongly developed in the biotite altered zones. Partial replacement of secondary and phenocrystic biotite by chlorite-magnetite ± illite is associated with fine-grained intergrowths of chalcopyrite and/or pyrite. Feldspars have been altered to illite ± quartz ± chlorite (Figs. 6C, D, 7). In the andesite, where pervasive biotite alteration is strongest, intermediate argillic alteration has produced clots of chlorite-illite ± quartz ± muscovite. Related ore mineralization includes veins and veinlets of chalcopyrite-quartz-anhydrite with prominent chlorite-illite selvages (Figs. 6E, F, 7). These veins are cut by illite-pyrite-quartz ± anhydrite veins and late pyrite-calcite-chlorite ± quartz ± anhydrite veins. Similar veins occur in the outer phyllic and propylitic zones, where pyrite is the dominant sulfide.

The phyllic alteration (stage 4; Table 1) changes in mineralogy from early muscovite- to late-stage illite-dominant assemblages. Crosscutting relationships observed at the periphery of the deposit during this study show that phyllic alteration overprinted the intermediate argillic and propylitic alteration assemblages. Phyllic alteration destroyed primary rock textures totally, producing domains of illite-muscovite ± carbonate ± chlorite. Clots of illite-chlorite ± carbonate ± hematite ± muscovite (phengite) occur in a zone transitional to the central zone of potassic alteration. Blades of muscovite up to 0.5 mm long form radial intergrowths. Fine-grained pyrite and chalcopyrite are disseminated throughout the phyllic alteration zone. However, chalcopyrite is absent where the rock is intensely altered by phyllic assemblages. Illite-chlorite clots are common in the deepest parts of the late dacitic porphyries, where they are associated with partial replacement of the feldspars by illite-muscovite.

The highest copper grades coincide with regions of abundant chalcopyrite-quartz ± magnetite ± biotite ± K-feldspar

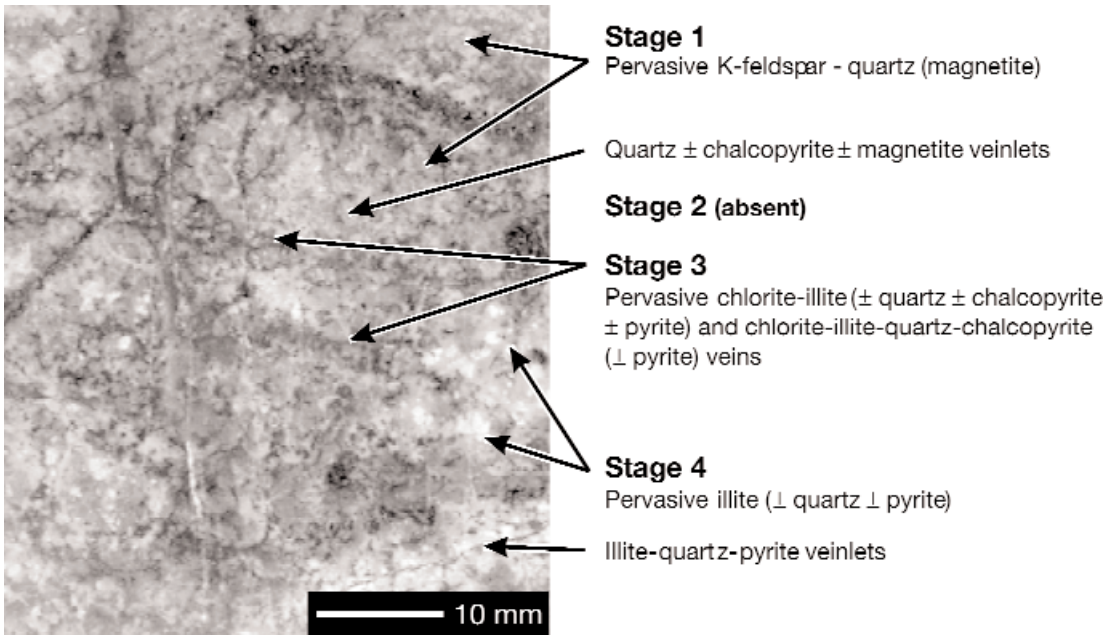


FIG. 7. Representative sample of P2 Porphyry, showing the alteration stages in the central parts of the Bajo de la Alumbrera deposit. The feldspathic groundmass of this intrusive phase has been largely replaced by K-feldspar and quartz (giving the typically gray porphyry a pinkish tint). Fine-grained disseminated magnetite occurs throughout this pervasive potassic alteration assemblage (stage 1). Also associated with the potassic alteration are thin quartz ± chalcopyrite ± magnetite veinlets. Intermediate argillic alteration (stage 3) overprints and cuts the potassic assemblage. This alteration is seen as veins and clots that comprise chlorite-illite ± quartz. Chalcopyrite and pyrite veins associated with this assemblage have a distinct alteration selvage of chlorite and illite. Finally, phyllic alteration (stage 4) occurs as the pervasive replacement of the already altered groundmass and a crosscutting pyrite (and lesser chalcopyrite) vein with a selvage of illite.

veins (late potassic alteration overprint) and zones of pervasive biotite alteration (Proffett, 2003). Some of these copper-rich zones occur in regions affected, in part, by chlorite-illite ± rutile ± magnetite (intermediate argillic) alteration. The highest gold grades coincide with the highest copper concentrations (Proffett, 2003). Most of the ore occurs in the P2 and the Early P3 porphyry (Ulrich, 1999; Ulrich and Heinrich, 2002; Ulrich et al., 2002; Proffett, 2003). Much lower copper-gold grades occur in the later porphyries (e.g., Late P3).

Previous radiometric age determinations of the potassic alteration assemblages range from 7.10 ± 0.13 to 6.83 ± 0.07 Ma (Sasso and Clark, 1998). These analyses were of altered biotite in two porphyritic intrusions. Sasso (1997) reported an age of 6.75 ± 0.09 Ma for pervasively developed phyllic alteration assemblages. These ages, when compared to the magmatic ages given by zircon $^{206}Pb/^{238}U$, suggest that hydrothermal activity may have continued for a few hundred thousand years (Harris et al., 2004b).

## Sampling and Methods

Vein material for fluid inclusion and stable isotope analyses was sampled from the Bajo de la Alumbrera mine workings and drill core (App. Fig. A1). Fluid inclusions were studied from quartz in each vein and alteration assemblage using polished sections. Microthermometry measurements were conducted on a Linkam THMSG 600 heating-freezing stage (University of Queensland) at 1 atm, calibrated with synthetic fluid inclusions produced by Syn Flinc. Measurements below 10°C are accurate to within ±0.1°C, and measurements above this temperature to within ±1°C. High-temperature (>600°C) homogenization measurements were performed using a LINKAM TS1500 heating stage (University of Tasmania). At high temperatures, the uncertainty may be up to 20°C. Microthermometric observations were mostly made on primary inclusions occurring in apparent growth zones in individual vein quartz crystals. A limited number of secondary fluids were studied from microfractures in the zones of most intense pervasive phyllic alteration. All temperatures reported here are uncorrected for pressure, and therefore homogenization temperatures are probably lower by tens of degrees than the true trapping temperature (see Eastoe, 1978).

Calculations of salinity from ice-melting temperatures were made assuming an NaCl-$H_2O$ system as modeled by Bodnar (1994). Salinity for brine inclusions (including those that are polyphase) was calculated using the equations of Bodnar and Vityk (1994) from the dissolution temperature of halite and assumes a simple NaCl-$H_2O$ system. Salinity is reported as weight percent NaCl equiv.

Nearly pure mineral separates for stable isotope analyses were prepared by microdrilling phyllosilicates (biotite, muscovite, chlorite, and illite), and the mineralogy was confirmed by standard petrographic microscopy and from spectra measured using a portable short wavelength infrared field spectrometer. Quartz separates were crushed to coarse sand and cleaned of sulfides. Water for $\delta D$ determinations was extracted from phyllosilicate minerals and fluid inclusions in quartz by stepwise heating of the sample under vacuum. The extracted water was reduced to hydrogen by reaction with zinc metal at 450°C (Coleman et al., 1982). Quartz and phyllosilicate minerals selected for $\delta^{18}O$ analyses were reacted at 650°C with $BrF_5$ in nickel vessels to liberate oxygen, which was converted to $CO_2$ by reaction with an internally heated carbon rod (Clayton and Mayeda, 1963). Isotopic analyses were performed on a Micromass 602E mass spectrometer, which uses the dynamic gas flow method to compare gas from the unknown samples with a reference gas. All isotopic data are reported in per mil relative to Vienna standard mean ocean water. Analytical uncertainties are better than ±0.2 per mil ($1\sigma$) for silicate oxygen isotope analyses and ±3 per mil ($1\sigma$) for silicate and inclusion hydrogen isotope analyses. Measured isotopic values (Table 2) were normalized against an international standard through the repeat analysis of NSB 28 (+9.5‰ $\delta^{18}O$) and NSB 30 (–65‰ $\delta D$).

Although there are some doubts as to the usefulness of $\delta D$ values determined from fluid inclusions in vein quartz (Faure et al., 2002; Faure, 2003), we are confident that the results reported for quartz are not mixed isotopic compositions because of careful sample selection. We undertook isotopic analyses only on samples that were interpreted to have minimal overprinting by later alteration, based on detailed petrographic observations. This is most important for samples of the potassic alteration assemblages. We determined the modal abundance of fluid inclusions in the different alteration assemblages using the method of Sheets et al. (1996) and found that vein quartz associated with potassic alteration has between 2.0 and 2.5 vol percent of liquid inclusions. Typically this inclusion type is associated with the lower temperature alteration assemblages and, as such, could affect the results. However, as these inclusions are volumetrically minor compared to the larger and more abundant high-temperature brine inclusions, this effect is thought to be minimal. A few samples had up to 10 percent by volume of liquid-rich inclusions, but their measured isotopic compositions do not differ markedly from those of the coexisting phyllosilicate minerals.

## Fluid Inclusion Microthermometry

Ulrich et al. (2002) defined six fluid inclusion types at Bajo de la Alumbrera that can be grouped into three distinct classes (Fig. 8A-C): (1) vapor-rich inclusions with small chalcopyrite or hematite daughter minerals and variable vapor/liquid ratios (<20 vol % liquid); (2) liquid-rich aqueous (<40 vol % vapor) inclusions with small chalcopyrite or hematite daughter minerals; (3) brine inclusions with numerous

TABLE 2. Summary of Isotope Fractionation Equations Used in This Study

| Element fractionation equation | Reference |
|---|---|
| Oxygen | |
| $10^3 \ln \alpha_{albite-H_2O} = 2.39 \times 10^6 T^{-2} - 2.51$ | Matsuhisa et al. (1979) |
| $10^3 \ln \alpha_{biotite-H_2O} = 0.4 \times 10^6 T^{-2} - 3.1$ | Bottinga and Javoy (1973) |
| $10^3 \ln \alpha_{chlorite-H_2O} = 2.693 \times 10^9 T^{-3} - 6.342 \times (10^6) T^{-2} + 2.969 \times (10^3) T^{-1}$ | Cole and Ripley (1999) |
| $10^3 \ln \alpha_{illite-H_2O} = 2.39 \times 10^6 T^{-2} - 3.76$ | Sheppard and Gilg (1996) |
| $10^3 \ln \alpha_{magnetite-H_2O} = 1.47 \times 10^6 T^{-2} - 3.70$ | Bottinga and Javoy (1973) |
| $10^3 \ln \alpha_{quartz-H_2O} = 3.34 \times 10^6 T^{-2} - 3.31$ | Matsuhisa et al. (1979) |
| Hydrogen | |
| $10^3 \ln \alpha_{biotite-H_2O} = -21.3 \times 10^6 T^{-2} - 2.8$ | Suzuki and Epstein (1976) |
| $10^3 \ln \alpha_{chlorite-H_2O}$ (GRAPH, below 350°C) | Marumo et al. (1980) |
| $10^3 \ln \alpha_{illite-H_2O} = 25 \pm 5$ (between 120°–400°C) | Sheppard and Gilg (1996) |

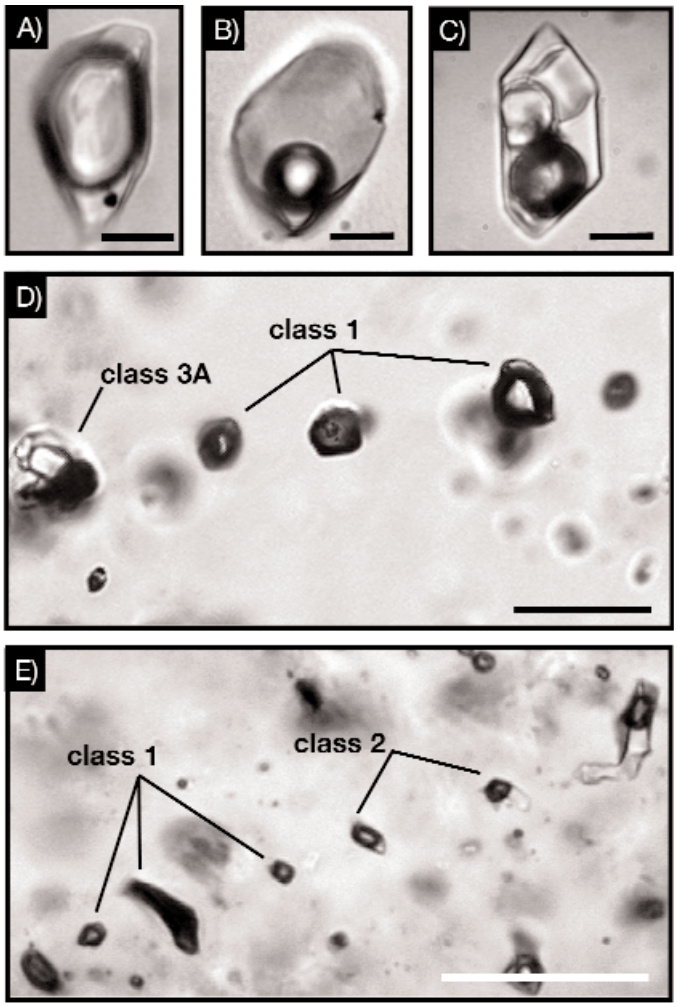


FIG. 8. Photomicrographs of fluid inclusions classes and coexisting fluid inclusion assemblages. A. Vapor-rich (class 1) inclusion with a single unidentified (chalcopyrite?) daughter mineral. B. Liquid-rich aqueous (class 2) inclusion with small chalcopyrite daughter crystal. C. Brine (class 3) inclusion with a distinct halite crystal and three other unidentified daughter crystals, including an opaque phase. D. Coexisting polyphase brine (class 3A) and vapor-rich (class 1) inclusions occurring in primary inclusion trail found in hydrothermal quartz. The crystal is from a quartz-chalcopyrite ± biotite-K-feldspar vein (potassic alteration assemblage) that cuts the P2 Porphyry. E. Coexisting vapor-liquid (class 1) and vapor-rich (class 2) fluid inclusions occurring in hydrothermal quartz from a quartz-pyrite ± illite vein (phyllic alteration assemblage) that cuts P2 Porphyry. This is a primary inclusion trail that runs parallel to the pyrite-filled core of the vein.

daughter minerals including chalcopyrite or hematite. Class 3 inclusions can be further divided into polyphase brine (3A) and simple brine inclusions (3B), depending on the number of daughter crystals. This terminology is applied here.

*Biotite-K-feldspar (potassic) alteration assemblage*

Fluid inclusions occurring in veins associated with potassic alteration assemblages are characterized by chalcopyrite-magnetite–bearing class 3A and lesser vapor rich class 1 inclusions (Fig. 8D; Ulrich et al., 2002). Homogenization temperatures reported by Ulrich et al. (2002) for inclusions associated with potassic alteration assemblages are ≥ 500° and reach 730°C, with salinities between 68 and 32 wt percent NaCl equiv. Our observations of 35 inclusions in mineralized potassic alteration assemblages found homogenization temperatures (typically by vapor disappearance) between 550° and 300°C. Our calculated salinities range from 57 to 25 wt percent NaCl equiv in the brine inclusions (Fig. 9), whereas high-density vapor inclusions in the same assemblage have salinities up to 10 wt percent NaCl equiv.

Microthermometry of fluid inclusions in quartz-magnetite veins that are temporally associated with potassic alteration assemblages highlights several generations of veins. There is a systematic temporal and spatial separation of high-temperature fluid inclusions from lower temperature and salinity inclusions, more typical of the potassic alteration assemblages. Some of the earliest veins (so-called P veins) have chalcopyrite-bearing class 3A inclusions that homogenize by vapor disappearance at temperatures up to 845°C ($n$ = 24, Fig. 9), as previously reported in Harris et al. (2003). Furthermore, these inclusions have high apparent salinities, up to 65 wt percent NaCl equiv (Fig. 9). Ulrich et al. (2002) showed that most quartz-magnetite veins are characterized by class 3 inclusions with homogenization temperatures from 730° to 530°C and salinities between 65 and 35 wt percent NaCl equiv No microthermometric measurements could be made on associated class 1 inclusions owing to their small liquid content (Fig. 8D). During this study we observed fluid inclusions with homogenization temperatures between 441° and 417°C ($n$ = 12) and salinities from 32 to 28 wt percent NaCl equiv in paragenetically later quartz-magnetite veins from the deepest part of the deposit (e.g., sample ACH9983; Fig. A1).

*Intermediate argillic and phyllic alteration assemblages*

No microthermometric results have been previously reported for intermediate argillic alteration at Bajo de la Alumbrera. Here we report microthermometric data for 97 inclusions in this alteration zone. Quartz veins associated with pervasive chlorite-illite ± chalcopyrite ± pyrite ± muscovite alteration contain only low-density vapor coexisting with liquid-rich inclusions. Homogenization of the liquid-rich inclusions occurs by vapor disappearance from 390° to 250°C, and these inclusions have low salinities (2.0–3.8 wt % NaCl equiv; Fig. 9). Fluid inclusions in pyrite-quartz-chlorite veins have homogenization temperatures between 390° and 290°C and ice-melting temperatures of –12.2° to –6.6°C, corresponding to salinities between 12.0 and 3.0 wt percent NaCl equiv. Secondary inclusion trails in the adjacent chloritic selvages of the veins have homogenization temperatures between 270° and 250°C and salinities between 3.0 and 3.5 wt percent NaCl equiv. Aqueous carbon dioxide in the hydrothermal fluids may have depressed the ice-melting temperatures (Hedenquist and Henley, 1985).

The phyllic alteration assemblage (illite-muscovite-pyrite-quartz ± anhydrite) at Bajo de la Alumbrera is broadly zoned with respect to fluid inclusion populations. A total of 203 inclusions were studied from the phyllic alteration assemblages. Class 1 and 2 inclusions characterize the innermost assemblages and have homogenization (vapor disappearance) temperatures between 410° and 300°C and salinities from 3.2 to 4.1 wt percent NaCl equiv (Fig. 9). Several generations of the illite-muscovite-quartz-pyrite ± chlorite veins occur at the

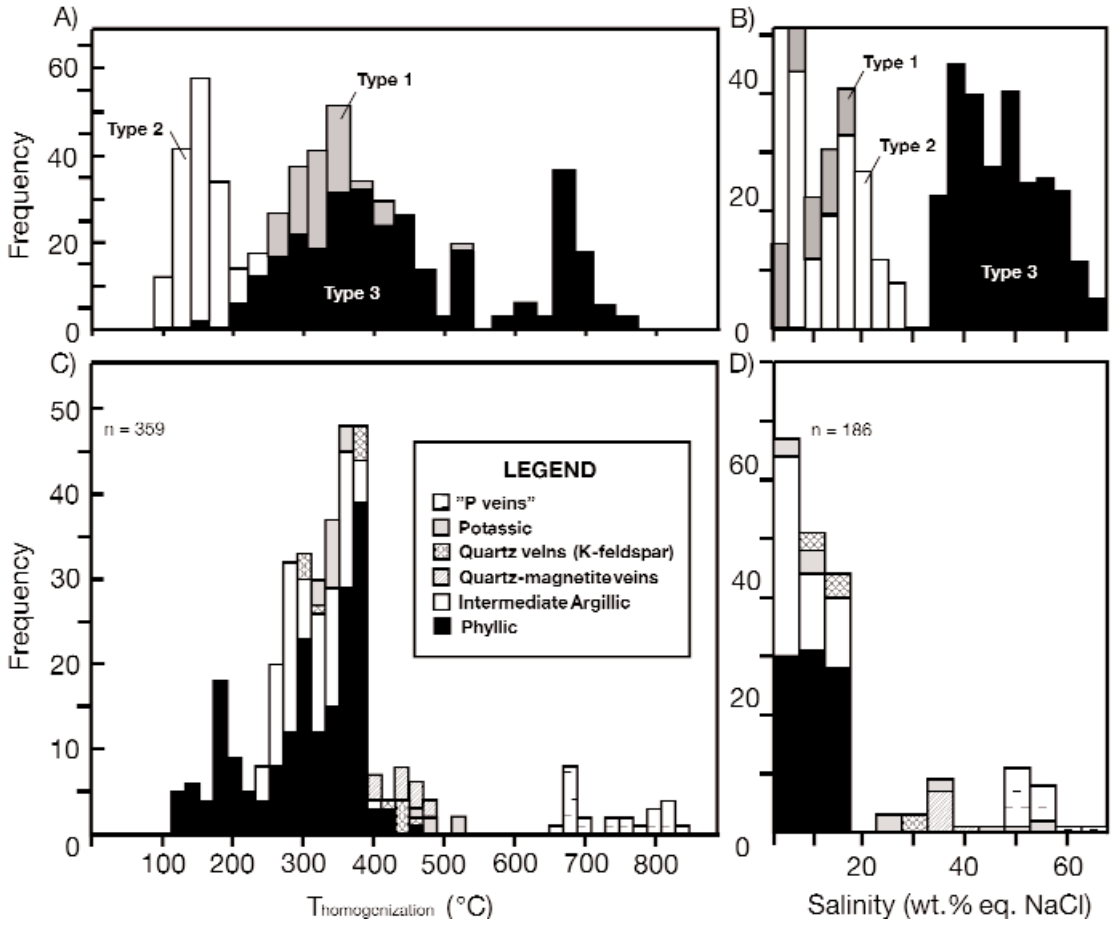


FIG. 9. Fluid inclusion data for the Bajo de la Alumbrera deposit. A. Compilation of the total homogenization data reported by Ulrich et al. (2002). Vapor-rich inclusions (type 1) coexist with brine inclusions (type 3) and occur in potassic alteration assemblages, whereas the liquid-rich (or aqueous) inclusions (type 2) occur in the overprinting phyllic alteration assemblages (Ulrich et al., 2002). B. Salinity data of Ulrich et al. (2002). C. New total homogenization data from this study subdivided by alteration assemblages. D. New salinity data for individual alteration assemblages.

periphery of the deposit. The earliest of these veins contain assemblages of vapor-liquid and low-density vapor inclusions (Fig. 8E) with homogenization temperatures (330°–300°C) and salinities (2.8–3.4 wt % NaCl equiv) similar to those in the pervasive intermediate argillic alteration in the core of the deposit.

We found trails of coexisting vapor-liquid and vapor-rich (~10 vol % liquid) fluid inclusions, inferred to be produced by boiling, with variable salinities (up to 15 wt % NaCl equiv) and homogenization temperatures (up to 380°C). Inclusions in later illite-quartz-anhydrite ± pyrite ± chalcopyrite and late pyrite-calcite-chlorite ± quartz ± anhydrite veins have progressively lower homogenization temperatures (200°–170°C) and variable salinities (3.8–4.1 wt % NaCl equiv), with the outermost zones having the lowest homogenization temperatures and salinities in the deposit (200°–130°C and 2.3–3.7 wt % NaCl equiv). Fluid inclusion assemblages showing evidence of boiling in the later vein generations have homogenization temperatures between 210° and 120°C and coexisting, moderately saline (10–15 wt % NaCl equiv) and low-salinity (<2 wt % NaCl equiv) inclusions. Although the measured temperatures are below the stability of illite (i.e., ~220°C: Reyes, 1990), smectite was not identified in the samples analyzed using the field spectrometer.

## Oxygen And Hydrogen Isotopes

We measured the $\delta^{18}O$ and $\delta D$ values of phyllosilicate minerals (biotite, chlorite, illite) and the $\delta^{18}O$ of quartz and $\delta D$ of water extracted from fluid inclusions in quartz in the main alteration stages at Bajo de la Alumbrera. The new isotopic data, combined with the results of Ulrich et al. (2002), are presented in Table 3. Temperature estimates from fluid inclusion homogenization data allow the isotopic compositions of the hydrothermal fluids responsible for successive alteration assemblages to be determined.

### *Igneous minerals*

Measured isotopic compositions of phenocrystic biotite from the Late P3 Porphyry range from +6.2 to +7.1 per mil $\delta^{18}O$ ($n$ = 3) and from –87 to –103 per mil $\delta D$ ($n$ = 2). Assuming a minimum solidus temperature of 700°C, the calculated $\delta D$ and $\delta^{18}O$ of water in equilibrium with the biotite

ranges from –62 to –78 and +8.9 to +9.8 per mil, respectively. These calculated water compositions match those reported by Ulrich et al. (2002) for phenocrystic quartz and biotite (i.e., +9.0 and –85‰, respectively). The $\delta$D values are lower than those of water dissolved in felsic magmas (Fig. 10A; Taylor, 1992). By contrast, the $\delta^{18}$O values are typical of melt compositions at these temperatures and are tightly clustered. The low $\delta$D values imply that the biotite in the late-stage porphyries (i.e., Late P3 and Late porphyries) formed from melts that had already exsolved significant volumes of water (Taylor, 1986).

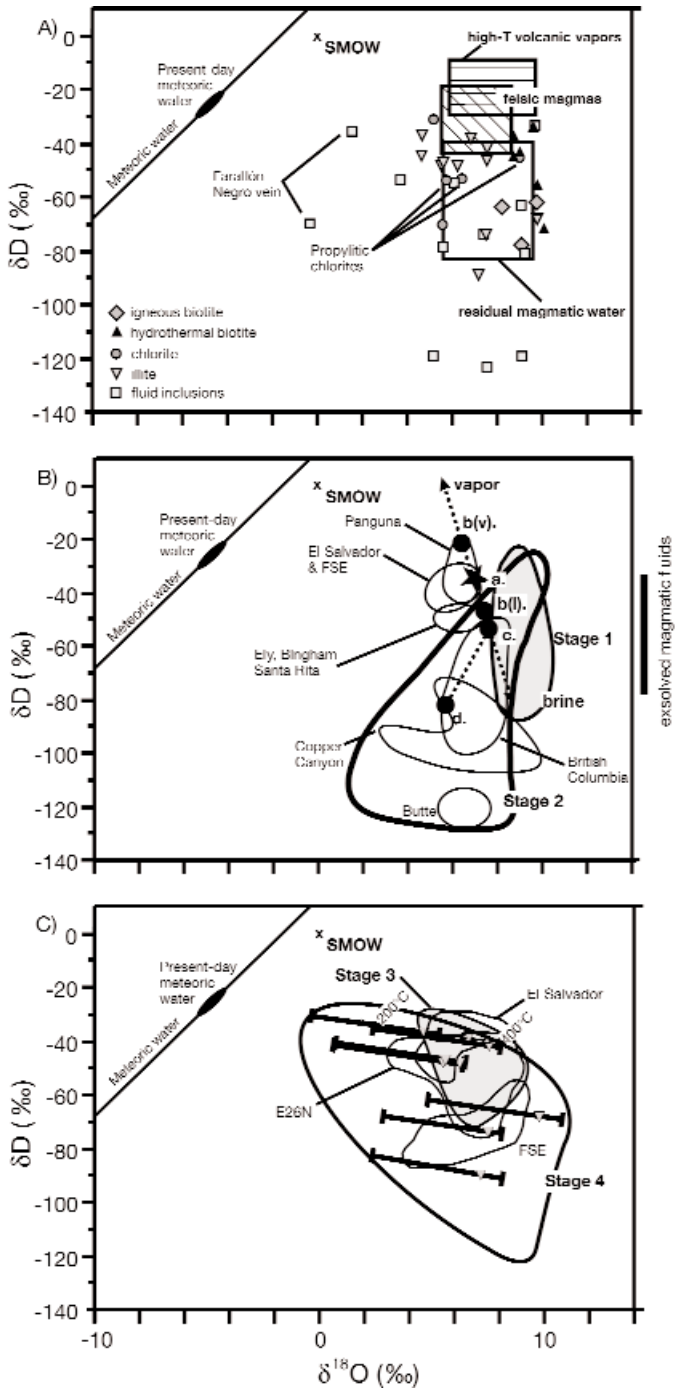


*Potassic alteration minerals*

Measured $\delta^{18}$O and $\delta$D values of hydrothermal biotite from the earliest potassic alteration assemblages at Bajo de la Alumbrera (stage 1) range from +6.4 to +7.5 and –72 to –102 per mil ($n$ = 3), respectively (Table 3). Associated vein quartz has $\delta^{18}$O values between +9.9 and +10.6 per mil ($n$ = 3) and $\delta$D values of fluid inclusion water that range from –33 to –81 per mil ($n$ =3). Our quartz $\delta^{18}$O values are consistent with those previously reported by Ulrich et al. (2002; i.e., +10.5 to +10.6‰, $n$ = 2). Ulrich et al. (2002) also reported magnetite $\delta^{18}$O values between +2.8 and +3.1 per mil.

Based on all available data (including those of Ulrich et al., 2002), the calculated and/or measured isotopic compositions of hydrothermal fluids responsible for the early high-temperature potassic alteration range from $\delta^{18}$O values of +8.1 to +10.4 per mil and $\delta$D values of –33 to –81 per mil. The compositions were calculated based on the available fluid inclusion data indicating temperatures of formation between 550° and 700°C (Ulrich et al., 2002; this study) and plot in or immediately adjacent to the composition of magmatic fluids (Fig. 10A; Taylor et al., 1979).

Our measured $\delta^{18}$O values of vein quartz in alteration assemblages associated with the bulk of the mineralization (stage 2) range from +8.3 to +10.6 per mil ($n$ = 4), which are similar to those reported by Ulrich et al. (2002; i.e., between +8.5 and +11.3‰, $n$ = 4). Our $\delta$D values for water extracted from fluid inclusions range from –74 to –123 per mil ($n$ =3). Ulrich et al. (2002) reported $\delta^{18}$O and $\delta$D values for hydrothermal biotite and whole-rock samples of pervasive biotite alteration assemblages, which range from +6.5 to +7.4 ($n$ = 3) and –68 to –90 per mil ($n$ = 5), respectively.

FIG. 10. A. Calculated $\delta^{18}$O and $\delta$D values of fluids responsible for different alteration assemblages at the Bajo de la Alumbrera porphyry copper-gold deposit (includes recalculated data from Ulrich et al., 2002). Compositions are based on model fluid temperatures determined from fluid inclusion data. Ranges of residual magmatic water (i.e., that remaining in an intrusion after degassing and crystallization: Taylor, 1974), compositions of water initially dissolved in felsic melts (Taylor, 1992), and low-salinity vapor discharges from high-temperature volcanic fumaroles (Giggenbach, 1992) are also shown and discussed in the text. B. Isotopic compositions of fluids associated with potassic alteration (modified after Hedenquist et al., 1998). Fluid compositions associated with early (stage 1) and late (stage 2) potassic alteration at Bajo de la Alumbrera. Isotopic trends plotted here can be explained using numerical modeling (calculated after Shmulovich et al., 1999). From a primitive starting composition (point a), a magmatic fluid evolves during phase separation or boiling to distinctly different isotopic compositions. Point b(v) and b(l) mark the resultant vapor and liquid compositions, respectively. Cooling of the brine liquid causes further modification of the primitive magmatic signature resulting in depleted hydrogen and oxygen isotope compositions (point c). If a new pulse of unevolved magmatic fluid is introduced into the system, the hotter magmatic fluid will flash and drive fractionation to a maximum (point d; see text for explanation). Note the overlap of the isotopic compositions of fluid responsible for the stage 2 potassic alteration with those determined from other porphyry ore deposits (modified after Hedenquist and Richards, 1998). C. Isotopic compositions of fluids associated with intermediate argillic (stage 3) and phyllic (stage 2) alteration at Bajo de la Alumbrera. Compositional ranges for fluids associated with phyllic alteration are based on model fluid temperatures determined from inclusion data (i.e., between 200° and 400°C) and overlap with isotopic fluid compositions determined from other porphyry ore deposits (Hedenquist et al., 1998, Watanabe and Hedenquist, 2001; Harris and Golding, 2002).

TABLE 3. Oxygen and Hydrogen Isotopes from Alteration and Magmatic Minerals at Bajo de la Alumbrera

| Sample | Location | Mineral | Temperature[1] (°C) | T model (°C) | Measured[2] | | Calculated range[3] | | Model composition[3] | |
|---|---|---|---|---|---|---|---|---|---|---|
| | | | | | $\delta^{18}$O mineral | $\delta$D mineral | $\delta^{18}$O fluid | $\delta$D fluid | $\delta^{18}$O fluid | $\delta$D fluid |
| Stage 1 early potassic alteration | | | | | | | | | | |
| ACH0125 | GR. –66°36'30.708 –27°19'41.88 | Quartz | 550–700 | 625 | 9.9 | –62 | 8.3 to 9.7 | –62 | 9.1 | –62 |
| ACH99105 | DDH49.2-46.3; 143m | Quartz | | | 10.6 | –33 | 9.0 to 10.4 | –33 | 9.8 | –33 |
| ACH9984 | DDH49-50.1; 75m | Biotite | | | 7.5 | –102 | 10.0 to 10.2 | –68 to –77 | 10.1 | –73 |
| ACH9985 | DDH50.46.43; 613.2m | Biotite | | | 7.2 | –84 | 9.7 to 9.9 | –50 to –59 | 9.8 | –55 |
| ACH9987 | DDH49.64.3; 690m | Biotite | | | 6.4 | –72 | 8.9 to 9.1 | –38 to –47 | 9.0 | –43 |
| ACH9983 | DDH49-64.3; 754m | Quartz | | | 10.2 | –81 | 8.6 to 10.0 | –81 | 9.4 | –81 |
| 40-60/93 | DDH49-60; 93.0m | Quartz[4] | | | 10.6 | N.D. | 9.0 to 10.4 | N.D. | 9.8 | N.D. |
| 40-60/93 | DDH49-60; 93.0m | Magnetite[4] | | | 3.1 | N.D. | 8.4 to 9.0 | N.D. | 8.6 | N.D. |
| 49-61.4/357 | DDH49-61.4; 336.0m | Quartz[4] | | | 10.5 | N.D. | 8.9 to 10.3 | N.D. | 9.7 | N.D. |
| 49-61.4/357 | DDH49-61.4; 336.0m | Magnetite[4] | | | 2.8 | N.D. | 8.1 to 8.7 | N.D. | 8.3 | N.D. |
| Stage 2 late potassic alteration | | | | | | | | | | |
| ACH9973 | DDH 48.5-54; 139 m | Quartz | 300–550 | 450 | 10.6 | –123 | 3.7 to 9.0 | –123 | 7.5 | –123 |
| ACH9999 | DDH 51-56; 52m | Quartz | | | 10.4 | –74 | 3.5 to 8.8 | –74 | 7.3 | –74 |
| ACH99153 | DDH 49.2-46.3; 446m | Quartz | | | 9.7 | N.D. | 2.8 to 8.1 | N.D. | 6.6 | N.D. |
| ACH99157 | DDH 47-64.3; 794m | Quartz | | | 8.3 | –119 | 1.4 to 6.7 | N.D. | 5.2 | –119 |
| 51-52.2/308 | DDH51-52.2; 308.7m | Biotite[4] | | | N.D. | –68 | | 0 to –34 | N.D. | –24 |
| 51-52.2/308 | DDH51-52.2; 308.7m | Quartz[4] | | | 8.5 | N.D. | 1.6 to 6.9 | N.D. | 5.4 | N.D. |
| 49.2-46.3/452 | DDH49.2-46.3; 264.6m | Biotite[4] | | | N.D. | –80 | | –12 to –46 | N.D. | –36 |
| 49.2-46.3/452 | DDH49.2-46.3; 264.6m | Quartz[4] | | | 9.7 | N.D. | 2.8 to 8.1 | N.D. | 6.6 | N.D. |
| BLA97 | Surface sample | Quartz[4] | | | 11.3 | N.D. | 4.4 to 9.7 | N.D. | 8.2 | N.D. |
| 49-61.4/94 | DDH49-61.4; 94.0m | Biotite[4] | | | 7.4 | –79 | 9.3 to 9.9 | –11 to –45 | 9.7 | –35 |
| 37-49/275 | DDH37-49; 275.0m | Biotite[4] | | | 6.5 | –90 | 8.4 to 9.0 | –22 to –56 | 8.8 | –46 |
| 37-49/275 | DDH37-49; 275.0m | Biotite[4] | | | 6.5 | –83 | 8.4 to 9.0 | –15 to –49 | 8.8 | –39 |
| 43-47.1/195 | DDH43-47.1; 195m | Quartz[4] | | | 9.2 | –55 | 2.3 to 7.6 | –55 | 6.1 | –55 |
| Propylitic alteration | | | | | | | | | | |
| BAL00/263 | GR. –66°36'36.0648 –27°19'24.456 | Chlorite | 300–375 | 325 | 8.8 | –69 | 8.6 to 9.4 | N.D. | 9.0 | –45 |
| BLA55 | Surface sample | Chlorite[4] | | | N.D. | –77 | - | N.D. | N.D. | –53 |
| BLA55 | Surface sample | Albite[4] | | | 10.6 | N.D. | 5.8 to 7.4 | N.D. | 6.4 | N.D. |
| BLA64 | Surface sample | Chlorite[4] | | | N.D. | –78 | - | N.D. | N.D. | –54 |
| BLA64 | Surface sample | Albite[4] | | | 9.9 | N.D. | 5.1 to 6.7 | N.D. | 5.7 | N.D. |
| Stage 3 intermediate argillic alteration | | | | | | | | | | |
| ACH9987 | DDH49.64.3; 690m | Chlorite | 300–375 | 325 | 5.0 | –55 | 4.8 to 5.6 | N.D. | 5.2 | –31 |
| ACH0125 | GR. –66°36'30.708 –27°19'41.88 | Chlorite | | | 7.5 | –95 | 7.3 to 8.1 | N.D. | 7.7 | –71 |

TABLE 3. *(Cont.)*

| Sample | Location | Mineral | Temperature[1] (°C) | T model (°C) | Measured[2] | | Calculated range[3] | | Model composition[3] | |
|---|---|---|---|---|---|---|---|---|---|---|
| | | | | | $\delta^{18}$O mineral | $\delta$D mineral | $\delta^{18}$O fluid | $\delta$D fluid | $\delta^{18}$O fluid | $\delta$D fluid |
| Stage 4 main-stage phyllic alteration | | | | | | | | | | |
| ACH9923 | GR. –66°36'43.740 | | | | | | | | | |
| | –27°19'53.040 | Quartz | 200–400[5] | 375 | 13.7 | –119 | 2.1 to 9.6 | –119 | 9.1 | –119 |
| ACH9994 | DDH49.2-46.3; 106.0m | Quartz | | | 10.8 | N.D. | –0.8 to +6.7 | N.D. | 6.2 | N.D. |
| ACH99162 | DDH47.64.3; 849.6m | Illite | | | 10.6 | N.D. | 3.7 to 9.1 | N.D. | 8.7 | N.D. |
| ACH9986 | DDH47.64.3; 264.5m | Illite | | | 11.7 | –93 | 4.8 to 10.2 | –63 to –73 | 9.8 | –68 |
| ACH99150 | DDH49.2.46.3; 262.0m | Illite | | | N.D. | –91 | N.D.- | –61 to –71 | N.D. | –66 |
| ACH9994 | DDH49.2-46.3; 106.0m | Illite | | | 7.4 | –72 | 0.5 to 5.9 | –42 to –52 | 5.5 | –47 |
| ACH0101 | DDH51-45.2; 107.0m | Illite | | | 9.1 | –113 | 2.2 to 7.6 | –83 to –93 | 7.2 | –88 |
| ACH0103 | DDH51-45.2; 121m | Illite | | | 9.4 | –98 | 2.5 to 7.9 | –68 to –78 | 7.5 | –73 |
| ACH9983 | DDH49-64.3; 754m | Illite | | | 8.7 | –63 | 1.8 to 7.2 | –33 to –43 | 6.8 | –38 |
| ACH99102 | DDH48.4-54; 124.4m | Illite | | | 6.6 | –61 | –0.3 to +5.1 | –31 to –41 | 4.7 | –36 |
| ACH99151 | DDH49-50.1; 315.8m | Illite | | | 9.5 | –66 | 2.6 to 8.0 | –36 to –46 | 7.6 | –41 |
| ACH99154 | DDH 49.1-40; 710.0m | Illite | | | 7.5 | –72 | 0.6 to 6.0 | –42 to –52 | 5.6 | –47 |
| 49.2-46.3/1-2 | DDH49.2-46.3; 264m | Illite (?)[4] | | | N.D. | –71 | N.D.- | –41 to –51 | N.D. | –46 |
| 49.2-46.3/1-2 | DDH49.2-46.3; 264m | Quartz[4] | | | 10.3 | N.D. | –1.3 to +6.2 | | 5.7 | N.D. |
| 57.5-60/7 | DDH57.5-60; 51m | Illite (?)[4] | | | N.D. | –73 | N.D.- | –43 to –53 | N.D. | –48 |
| 57.5-60/7 | DDH57.5-60; 51m | Quartz[4] | | | 10.7 | N.D. | –0.9 to +6.6 | | 6.1 | N.D. |
| 46-42.5/1 | DDH46-42.5; 46m | Illite (?)[4] | | | N.D. | –69 | N.D.- | –39 to –49 | N.D. | –44 |
| 46-42.5/1 | DDH46-42.5; 46m | Quartz[4] | | | 10.7 | N.D. | –0.9 to +6.6 | | 6.1 | N.D. |
| 55.5-60/192 | DDH55.5-60; 192m | Quartz[4] | | | 8.3 | –52 | –3.3 to +4.2 | –52 | 3.7 | –52 |
| 38-49/97 | DDH38-49; 97m | Quartz[4] | | | 10.2 | –79 | –1.4 to +6.1 | –79 | 5.6 | –79 |
| Stage 5 sulfide-sulfate-carbonate veins | | | | | | | | | | |
| | N.D. | N.D. | | | N.D. | N.D. | | | | |
| Porphyritic intrusions | | | | | | | | | | |
| ACH9981 | DDH47-64.3; 786.5m | Biotite | | 700 | 6.4 | –103 | | | 9.1 | –78 |
| ACH9998 | DDH49.1-64; 770.9m | Biotite | | | 7.1 | –87 | | | 9.8 | –62 |
| ACH9972 | DDH49.1-64; 771.0m | Biotite | | | 6.2 | N.D. | | | 8.9 | N.D. |
| LP | Surface sample | Biotite[4] | | | N.D. | –110 | | | N.D. | –85 |
| LP | Surface sample | Quartz[4] | | | 9.2 | N.D. | | | 9.0 | |

Abbreviation: N.D. = no data

[1] Model temperature as determined from the fluid inclusion homogenization temperatures

[2] Analytical uncertainties are less than 0.2 per mil (1$\sigma$) for silicate oxygen isotope analyses and 3 per mil (1$\sigma$) for silicate and inclusion hydrogen isotope analyses

[3] Calculated $\delta^{18}$O and $\delta$D fluid composition determined using isotope fractionation equations listed in Table 2

[4] Data from Ulrich et al. (2002)

[5] Most empirical and experimental data for the deuterium fractionation factor of illite show that it is not very sensitive from 120° to 400°C (Sheppard and Gilg, 1996); therefore 400° and 120°C are used as the maximum and minimum temperature, respectively, in the modeling of the water compositions of intermediate argillic and phyllic alteration

Assuming an average temperature of 450°C, the calculated $\delta^{18}O$ and $\delta D$ of fluids related to ore-forming potassic stage alteration range from +5.2 to +9.7 and –24 to –123 per mil, respectively. The isotopic compositions of the fluids are similar to those associated with K-silicate alteration of other porphyry copper and copper-gold deposits, in that the bulk of the samples plot in the range of residual magmatic water (Fig. 10A). The $\delta^{18}O$ and $\delta D$ values are highly variable, and the fluids are depleted in D relative to the stage 1 fluids. This variation is more pronounced if the spectrum of observed homogenization temperatures (300°–550°C) from the stage of potassic alteration is used. The $\delta^{18}O$ values range from magmatic (+9.9‰) to more depleted compositions (+1.4‰; Table 3). The lower $\delta^{18}O$ values coincide with lower $\delta D$ values (–119 to –123‰). Although these compositions are shifted toward the meteoric water line, they do not trend toward values indicating involvement of meteoric water at the time of mineralization (see below).

*Propylitic alteration minerals*

One chlorite sample from the propylitic alteration assemblage was analyzed in this study, yielding a $\delta^{18}O$ value of +8.8 and a $\delta D$ value of –69 per mil. This adds to the two chlorite-albite pairs of Ulrich et al. (2002). Calculated fluid compositions of the peripheral propylitic alteration all plot in or just outside the residual magmatic water box (Fig. 10A). Calculated isotopic compositions are based on fluid inclusion homogenization temperatures ranging from 300° to 375°C and indicate $\delta^{18}O$ values from +8.6 to +9.4 ($n$ = 1) and $\delta D$ values from –45 to –54 per mil ($n$ = 3), respectively. A lower $\delta^{18}O$ value was calculated from the two albite samples analyzed by Ulrich et al. (2002; i.e., from +5.1 to +7.4‰).

*Intermediate argillic alteration minerals*

No isotopic analyses have been undertaken previously on this alteration assemblage. Measured $\delta^{18}O$ and $\delta D$ values of two chlorite samples range from +5.0 to +7.5 and –55 to –95 per mil, respectively. The calculated $\delta^{18}O$ and $\delta D$ of the fluid of +4.8 to +8.1 and –31 to –71 per mil, respectively, plot in or just outside the residual magmatic water box (Fig. 10A). These compositions were calculated using a temperature range of 300° to 375°C, based on homogenization temperatures from the highest temperature veins from this assemblage.

*Phyllic alteration minerals*

The phyllic alteration assemblage at Bajo de la Alumbrera has quartz with measured $\delta^{18}O$ and $\delta D$ values from +10.8 to +13.7 ($n$ = 2) and –119 per mil ($n$ = 1), respectively. Ulrich et al. (2002) determined slightly lower $\delta^{18}O$ (+8.3 to +10.7‰; $n$ = 5) and $\delta D$ (–52 to –79‰; $n$ = 2) from quartz. Illite in this zone has $\delta^{18}O$ and $\delta D$ values that range from +6.6 to +11.7 ($n$ = 9) and –61 to –113 per mil ($n$ = 9), respectively. Our illite $\delta D$ values overlap those previously determined by Ulrich et al. (2002; i.e., –69 to –73‰, $n$ = 3). The fluid inclusions in the phyllic alteration zone have trapping temperatures that range from 200° to 400°C, with a mode of 375°C. Calculated fluid compositions at this temperature plot in or adjacent to the residual magmatic water box (Fig. 10A), with $\delta^{18}O$ and $\delta D$ values for water in equilibrium with illite from –0.3 to +10.2 ($n$ = 9) and –31 to –93 per mil ($n$ = 12), respectively (Table 3).

When modeled at 375°C, the water compositions calculated from illite define two distinct groups. One group is relatively depleted in D (–66 to –88‰) and plots in the residual magmatic water box; a second group is more enriched in D (–36 to –48‰). The latter group has lower $\delta^{18}O$ values (+4.7 to +7.6‰) compared to the former that have $\delta^{18}O$ values ranging from +7.2 to +9.8 per mil. Modeling at a lower temperature (200°C) shows that the group with higher $\delta D$ values has $\delta^{18}O$ values that approach late Miocene meteoric water compositions. Geologic observations, fluid inclusion microthermometry, and isotopic systematics of phyllic alteration minerals suggest that these assemblages formed during several stages, and we interpret the phyllic alteration in terms of a two-stage process. The earlier and innermost phyllic alteration formed from high-temperature (400°–300°C) and low-salinity (2.8–4.1 wt % NaCl equiv) fluids. Overprinting phyllic alteration assemblages formed from lower temperature (down to at least 220°C consistent with illite stability (Reyes, 1990) and from more saline fluids (up to 15 wt % NaCl equiv).

*Meteoric water*

The isotopic composition of late Miocene meteoric water has been estimated from model compositions determined from alteration minerals found in the Farallón Negro-Alto de la Blenda epithermal vein, approximately 15 km west-northwest of Bajo de la Alumbrera (Fig. 2). Ulrich et al. (2002) reported $\delta^{18}O$ values of +11.7 per mil from quartz and $\delta D$ values of –70 per mil from water extracted from fluid inclusions. By contrast, we measured $\delta^{18}O$ values of +13.7 and $\delta D$ values –36 per mil. Although Ulrich et al. (2002) found a narrow range of homogenization temperatures (220°–191°C) and lower salinity (~0.4 wt % NaCl equiv) in fluid inclusions in the Farallón Negro-Alto de la Blenda vein, we observed greater variability in the homogenization temperatures (between 270°–120°C). Moreover, we found salinities up to 18 wt percent NaCl equiv. Such high salinities may, in part, reflect a magmatic component in the hydrothermal fluids responsible for these epithermal veins or, alternatively, saline ground water.

Based on a modeling temperature of 200°C (as used by Ulrich et al., 2002), the water responsible for alteration in the Farallón Negro-Alto de la Blenda vein had $\delta^{18}O$ values from –0.4 to +1.6 and $\delta D$ values from –35 to –70 per mil. This calculation used the fractionation factor of Zhang et al. (1989). The $\delta^{18}O$ values overlap magmatic values, whereas the $\delta D$ values are shifted several per mil toward the meteoric water line. Our sample thus yields calculated isotopic compositions that define a dilution trend between magmatic and present-day meteoric water compositions reported from the region (i.e., $\delta^{18}O$ = –5 and $\delta D$ = –30‰; International Atomic Energy Agency, 1999; see Ulrich et al., 2002). Moreover, these compositions overlap with lower temperature phyllic alteration compositions at Bajo de la Alumbrera.

## Discussion

We interpret that magmatic water and gases were largely responsible for both the potassic (K-feldspar- and biotite-rich

assemblages) and the temporally separate, overprinting intermediate argillic and phyllic (illite-chlorite-pyrite-quartz ± muscovite) alteration assemblages at Bajo de la Alumbrera. Ulrich et al. (2002) concluded that high-temperature (up to 750°C) and hypersaline (up to 68 wt % NaCl equiv) fluids were introduced early into the deposit (i.e., stages 1 and 2). More recent studies reveal even hotter fluids (as high as 845°C) in some of the most primitive vein stages (Harris et al., 2003). By contrast, fluid inclusions associated with intermediate argillic (stage 3) and phyllic (stage 4) alteration assemblages are characterized by liquid-rich inclusions with <20 vol percent vapor, but vapor-rich inclusions with <60 vol percent vapor also occur throughout. Typically, the intermediate argillic and phyllic alteration assemblages are interpreted to have formed from lower temperature (between 400°–200°C) and low-salinity (less than 15 wt % NaCl equiv) fluids. It is apparent that the phyllic alteration assemblages (stage 4) developed during two stages; an early relatively high temperature (400°–300°C) event that was overprinted by lower temperature (down to 200°C) alteration as the system waned. Based on these temperature estimates there are three possible explanations for the isotopic compositions of the hydrothermal fluids responsible for the successive alteration assemblages: evolving magmatic fluids with phase separation; fluid-rock interaction, including inheritance of the magmatic isotopic composition of the wall rock and finite reservoir effects; or mixing of two isotopically distinct fluids.

*Magmatic fluids and phase separation*

The coexistence of saline inclusions with vapor-rich liquid inclusions in the potassic alteration assemblage can be explained by phase separation from an originally homogeneous aqueous fluid, with salinity in the range of 2 to 10 wt percent NaCl equiv, which exsolved from the magma at pressures of 1 to 1.5 kbars (equiv to depths of 4–6 km at lithostatic pressure; Henley and McNabb, 1978; Candela and Holland, 1984; Candela, 1989; Cline and Bodnar, 1991). On ascending to the depth where the porphyry stock was emplaced and ore formed (lithostatic pressures between 0.5–0.7 kbars), the magmatic fluid should have intersected its solvus, forming immiscible liquid and vapor phases of contrasting density.

Isotopic fractionation is most pronounced during phase separation of hypersaline liquid from vapor (e.g., Horita et al., 1995). The effect of this process can be traced by modeling the evolution of an originally homogeneous magmatic fluid (e.g., Horita et al., 1995; Hedenquist et al., 1998; Shmulovich et al., 1999; Harris and Golding, 2002). From an initial fluid having a $\delta^{18}O$ value of +7.0 per mil, a $\delta D$ value of –35 per mil, and a salinity of ~10 wt percent NaCl equiv at 550°C (Fig. 10B), boiling results in a vapor that has an isotopic composition similar to that exsolved from volcanic fumaroles (Giggenbach, 1992; Shmulovich et al., 1999). Hydroxyl-bearing minerals formed through wall-rock reaction with this vapor have high $\delta D$ and low $\delta^{18}O$ values, whereas reactions with the separated brine have the opposite (Fig. 10B; Harris and Golding, 2002).

The earliest potassic alteration at Bajo de la Alumbrera (stage 1) has calculated fluid isotopic compositions that are tightly clustered and are typical of compositions accepted as being magmatic in origin (e.g., Taylor, 1974). It appears that these compositions represent the least evolved or most primitive hydrothermal fluids introduced into the deposit. Evidence for the primitive nature of these fluids comes from the overlap between the $\delta D$ values reported here and those found in miarolitic cavities (Fig. 10B; Taylor et al., 1979). These fluids exhibit compositions that are D depleted and $^{18}O$ enriched compared to water dissolved in felsic melts (Taylor, 1992), consistent with the results of numerical modeling (Shmulovich et al., 1999). We therefore conclude that the earliest alteration stages at Bajo de la Alumbrera acquired their isotopic composition from brines that originated from boiling of an originally homogeneous magmatic fluid. The lack of higher $\delta D$ and lower $\delta^{18}O$ values implies that the vapor escaped from the deposit. Boiling also would have caused cooling of the magmatic fluid and further modification of the isotopic composition.

Hedenquist et al. (1998) proposed that D-depleted fluids associated with potassic alteration are derived from magma degassing. Degassing has the net effect of depleting D in the residual magmatic fluid in response to a progressive decline in the amount of water contained in the magma (Taylor et al., 1983; Dobson et al., 1989). For example, the low $\delta D$ values of phenocrystic biotite from the late-stage porphyries (from –62 to –78‰) suggest that at Bajo de la Alumbrera the late-stage melts had exsolved a large proportion of their volatiles by the time the biotite crystallized. If the residual magmatic fluids cause potassic alteration the associated hydroxyl-bearing minerals would inherit similarly low $\delta D$ values (e.g., Taylor et al., 1983). Therefore, mechanisms such as magma degassing may explain some of the D-depleted mineral and fluid isotopic compositions in the late-stage potassic alteration assemblages (e.g., Meinert et al., 2003).

The later potassic alteration assemblage at Bajo de la Alumbrera (stage 2), although typically having magmatic $\delta^{18}O$ values (Fig. 10B), has hydrogen isotope compositions that are variably depleted in D (to as low as –123‰). Similarly depleted compositions have been found in potassic alteration fluids at other porphyry copper deposits. For example, Selby et al. (2001) found very low $\delta D$ values (–120 to –180‰) relative to typical residual magmatic values (–40 to –80‰; Taylor, 1974) in potassic alteration in porphyry copper deposits of the Yukon, Canada. These compositions have been interpreted to be the result of meteoric waters mixing with high-temperature, saline magmatic aqueous fluids, based on an apparent correlation of the stable isotope composition of hydrothermal minerals with the $\delta D$ of paleometeoric waters (e.g., Sheppard and Taylor, 1974; Dilles et al., 1992; Zaluski et al., 1994; Sheets et al., 1996).

Bajo de la Alumbrera has remained at nearly the same latitude and elevation since the late Miocene (Pardo-Casas and Molnar, 1987; Kleinert and Strecker, 2001), so paleometeoric waters probably had similar isotopic compositions to modern meteoric waters ($\delta^{18}O$ = –5.0‰ and $\delta D$ = –30.0‰). Figure 10 shows no mixing between this meteoric water and primitive magmatic fluids found in the felsic magmas. Instead, the trend is toward compositions that are D and $^{18}O$ depleted, requiring a different explanation.

Injection of new magmatic water into a compositionally evolved hydrothermal system also may explain the most D

depleted, stage 2 mineral and fluid isotopic compositions. The injection of high-temperature (>650°C) saline magmatic fluid into a cooling hydrothermal system (<400°C) may result in flashing of the mixed magmatic fluid to vapor and hypersaline brine, resulting in a large isotopic fractionation (Fig. 10B; Shmulovich et al., 1999). If the hypersaline magmatic hydrothermal fluid subsequently cools and evolves along the line of halite saturation, the maximum fractionation of –28 per mil in $\delta$D and +2 per mil in $\delta^{18}$O is attained (Fig. 10B; Shmulovich et al., 1999).

Calculated water compositions of intermediate argillic alteration assemblages and the earlier stage, higher temperature (400°–300°C) phyllic alteration also overlap with residual magmatic water compositions, implying the involvement of magmatic water in their formation. The direct involvement of magmatic fluids in the development of the early higher temperature phyllic alteration assemblages is implicit in the extremely D depleted compositions ($\delta$D = –119‰). The small compositional shifts to $^{18}$O-depleted compositions relative to the residual magmatic water box (i.e., less than 1‰) imply that the overall influence of meteoric water on the development of this alteration phase was minimal. These small shifts in the $\delta^{18}$O values could be attributed to fluid-rock interaction.

*Fluid-rock interactions*

The interaction of hydrothermal fluids with wall rocks can lead to a pronounced shift in the isotopic composition of the fluid, which will directly influence the composition of the resulting alteration minerals (Taylor, 1974). When a 500°C magmatic fluid, with initial $\delta^{18}$O value of 7.0 per mil infiltrates a volcanic rock with a $\delta^{18}$O value of 8.0 per mil, the net effect is that isotopic exchange shifts the composition of the feldspars in the rock to values that are more enriched in $^{18}$O (by ~1.0‰). Simultaneously the $\delta^{18}$O composition of the fluid becomes lighter due to mass-balance effects. At lower temperatures (300°C), this effect is more pronounced as the feldspar compositions become up to 4 per mil heavier (as anticipated by the fractionation factor of Matthews et al., 1983) and the fluid becomes increasingly depleted in $^{18}$O. Hydrothermal minerals that form by interaction with an evolved fluid can therefore have an $\delta^{18}$O composition lower than if they had precipitated directly from a primary magmatic hydrothermal fluid.

Finite reservoir effects can be linked to fluid-rock interaction processes (e.g., Pollard et al., 1991). For example, fluid focused along discrete pathways (i.e., fractures or faults) will experience a high water/rock regime within the channelway, whereas fluids that infiltrate the surrounding rock must have lower water/rock ratios. If the magmatic fluid had a $\delta^{18}$O composition of +7.0 per mil, the composition of the initial quartz precipitated from the fluid will be +11.1 per mil (using a fractionation factor of 4.06 at 400°C, Matsuhisa et al., 1979). Following quartz precipitation the fluid becomes depleted in $^{18}$O, which is recorded in hydrothermal alteration assemblages subsequently formed by that fluid. Fluid-rock interaction is implicit in the pervasive nature of feldspar-destructive phyllic alteration and its localization along fracture and fault zones at Bajo de la Alumbrera (Fig. 7). Based on $\delta$D values, a magmatic origin has been proposed for the earliest phyllic alteration at Bajo de la Alumbrera. The $\delta^{18}$O values of the most D depleted fluids (i.e., $\delta$D = –66 to –119‰) associated with the phyllic stage are only slightly higher, by up to 2.0 per mil, than fluids responsible for the associated pervasive illite alteration (Table 3, Fig. 10C). We attribute such small shifts in the $\delta^{18}$O value of the early higher temperature phyllic alteration to finite reservoir effects and/or fluid-rock interaction.

*Fluid mixing*

In their study at Bajo de la Alumbrera, Ulrich et al. (2002) concluded that fluid mixing was significant during phyllic alteration stages. Based on the results of our isotopic modeling across a range of temperatures, this mixing occurred during the latest stage of phyllic alteration (see Fig. 10C). A pronounced shift of up to 8 per mil in the $\delta^{18}$O values is found when we model these fluids from 325° down to 200°C. Thus, the highest $\delta$D fluid values (i.e., –38 to –47‰) associated with the lowest temperature (illite-bearing) phyllic alteration can be interpreted in terms of mixing between magmatic compositions and the expected isotopic composition of paleometeoric water (Fig. 10C).

There are insufficient data to conclude whether the propylitic alteration zone peripheral to the ore-bearing potassic alteration developed from heated meteoric water, magmatic hydrothermal fluids, or some mixture of the two. A mixing model appears unlikely because of the small $\delta^{18}$O shift, relative to residual magmatic water (Table 3, Fig. 10A). Fluid-rock interaction could have caused such shifts in isotopic compositions, and such reactions are known to have occurred throughout the deposit.

## Conclusions

At Bajo de la Alumbrera alteration was developed in and around multiple (up to six) dacite porphyries that were emplaced during two distinct intrusive events separated by about a million years (Harris et al., 2004b). Geologic observations combined with geochronologic data show that hydrothermal activity may have continued for a few hundred thousand years (Sasso and Clark, 1998; Ulrich and Heinrich, 2002; Ulrich et al., 2002; Proffett, 2003; Harris et al., 2004b), during which time the underlying magma chamber was probably repeatedly saturated with water (along with dissolved volatiles and metals) through the injection of new magma batches and repeated decompression related to venting of fluids. Calculated $\delta^{18}$O and $\delta$D values confirm a magmatic origin for the fluids associated with the alteration zones, including potassic (biotite-K-feldspar ± quartz) and intermediate argillic (chlorite-illite ± pyrite) alteration assemblages at Bajo de la Alumbrera.

The lowest $\delta$D values of fluids associated with potassic alteration reflect evolved isotopic compositions imposed by magma degassing and/or by the injection of new magmatic water into a compositionally evolved hydrothermal system. Initially, the exsolved magmatic fluid comprised high-temperature (up to 845°C) brines containing up to 68 wt percent NaCl equiv and coexisting low-density vapor (Ulrich et al., 2002; Harris et al., 2003). This fluid had high $a_{(K^+)}/a_{(H^+)}$ that stabilized K-feldspar and biotite down to ~450°C. Decompression and cooling of the magmatic fluid have been suggested as possible mechanisms for ore deposition in earlier

studies (Ulrich et al., 2002; Harris et al., 2003; Proffett, 2003). Based on variations in $\delta^{18}O$ and $\delta D$ values of potassic alteration fluids, we conclude that early cooling of the magmatic fluid was largely a result of phase separation, producing coexisting brine and vapor-rich fluid inclusions.

Isotope geochemistry indicates that magmatic fluids were responsible for intermediate argillic alteration assemblages associated with copper-iron sulfide mineralization. This chlorite-illite ± pyrite alteration extends outward into phyllic assemblages (quartz-muscovite/illite ± pyrite) and developed during two stages. The direct involvement of magmatic fluids in the earliest higher temperature (between 400°–300°C) phyllic alteration is implied by the low $\delta D$ values (–66 to –119‰) coupled with moderately high $\delta^{18}O$ values (7.2–9.8‰). Fluids exsolved late in the magmatic cycle had lower salinity and may not have intersected their solvus (Hedenquist et al., 1998), thus retaining their original salinity (~2–4 wt % NaCl equiv). A decrease in temperature, a shift in $a_{(K^+)}/a_{(H^+)}$, and/or a decline in the total ion concentration or ionic strength of the fluid led to muscovite and then illite becoming the predominant K-silicate phase (e.g., Sverjensky et al., 1991; Hemley and Hunt, 1992). Fluid-rock interactions and finite reservoir effects explain the observed variations in the $\delta^{18}O$ of the earliest phyllic alteration.

Deposition of copper minerals took place over a wide range of temperatures from the early potassic alteration (over 400°C) to intermediate argillic alteration (from 400° to 200°C) and possibly lower. Conductive cooling is a slow mechanism for dissipation of heat and would have been even less effective here because each batch of fluid would have infiltrated a rock column already heated by earlier fluids. Fluid inclusion evidence indicates that phase separation (boiling) was important and likely the main cause of heat loss and possibly ore deposition (e.g., Hezarkhani and Williams-Jones, 1998). Our fluid inclusion observations demonstrate that boiling occurred in all fluids, including the relatively late stage fluids associated with phyllic alteration. The widely variable salinities found in these fluids (up to 15 wt% NaCl equiv) have been interpreted by Ulrich et al. (2002) to indicate the mixing of meteoric water into the system. Our modeling of stable isotope data suggests that dilution of the magmatic fluid system by meteoric water only occurred during the waning stages of the hydrothermal system, after it had cooled through 200°C, and long after the main stage of copper mineralization.

## Acknowledgments

We thank MIM Exploration and Minera Alumbrera for financial and logistic support. Special thanks to R. Valenta, P. Symons, D. Keough, S. Brown, and L. Rivera. J. Proffett and T. Ulrich are thanked for sharing their knowledge of Bajo de la Alumbrera. M. Alderete from Yacimientos Mineros Agua de Dionisio (YMAD) is thanked for granting initial access to the Farallón Negro district. P. Colls and K. Baublys provided specialized laboratory expertise, which has been critical to this project. This project was part of the senior author's Ph.D. and was supported by an Australian postgraduate scholarship. The senior author would like to thank T. Ulrich for helpful discussion during the earliest stages of this research. The manuscript was greatly improved because of discussions and reviews by J. Proffett, D. Cooke, T. Ulrich, Y. Watanabe, M. Solomon, and M. Hannington. Thanks to R. Large and numerous others at the Centre of Excellence in Ore Deposits (CODES) who made the completion of this manuscript possible.

*August 4, 2004; July 15, 2005*

## REFERENCES

Ahmad, S.N., and Rose, A.W., 1980, Fluid inclusions in porphyry and skarn ore at Santa Rita, New Mexico: Economic Geology, v. 75, p. 229–250.

Batchelder, J., 1977, Light stable isotope and fluid inclusion study of the porphyry copper deposit at Copper Canyon, Nevada: Economic Geology, v. 72, p. 60–70.

Beane, R.E., and Titley, S.R., 1981, Porphyry copper deposits. Part II. Hydrothermal alteration and mineralization: Economic Geology 75th Anniversary Volume, p. 235–269.

Bodnar, R.J., 1994, Synthetic fluid inclusions: XII. The system $H_2O$-NaCl: Experimental determination of the halite liquidus and isochores for a 40 wt % NaCl solution: Geochimica et Cosmochimica Acta, v. 58, p. 1053–1063.

Bodnar, R.J., and Vityk, M.O., 1994, Interpretation of microthermometric data for $H_2O$-NaCl fluid inclusions, *in* DeVivo, B., and Frezzotti, M.L., eds., Fluid inclusions in minerals: Methods and applications: Blacksburg, VA, Virginia Polytechnic Institute and State University, p. 117–130.

Bottinga, Y., and Javoy, M., 1973, Comments on oxygen isotope geothermometry: Earth and Planetary Science Letters, v. 20, p. 250–265.

Caelles, J.C., Clark, A.H., Farrar, E., McBride, S.L., and Quirt, S., 1971, Potassium-argon ages of porphyry copper deposits and associated rocks in the Farallón Negro-Capillitas district, Catamarca, Argentina: Economic Geology, v. 66, p. 961–964.

Candela, P.A., 1989, Felsic magmas, volatiles, and metallogenesis: Reviews in Economic Geology, v. 4, p. 223–233.

Candela, P.A., and Holland, H.D., 1984, The partitioning of copper and molybdenum between silicate melts and aqueous fluids: Geochimica et Cosmochimica Acta, v. 48, p. 373–380.

Clark, A.H., Farrar, E., Caelles, J.C., Haynes, S.J., Lortie, R.B., McBride, S.L., Quirt, G.S., Robertson, R.C.R., and Zentilli, M., 1976, Longitudinal variations in the metallogenetic evolution of the Central Andes; a progress report, *in* Strong, D.F., Metallogeny and plate tectonics: Geological Association of Canada Special 14, p. 23–58.

Clayton, R.N., and Mayeda, T.K., 1963, The use of bromine pentafluoride in the extraction of oxygen from oxides and silicates for isotopic analysis: Geochimica et Cosmochimica Acta, v. 27, p. 43–52.

Cline, J.S., and Bodnar, R.J., 1991, Can economic porphyry copper mineralization be generated by a typical calc-alkaline melt?: Journal of Geophysical Research, sec. B, v. 96, p. 8113–8126.

Cole, D.R., and Ripley, E.M., 1999, Oxygen isotope fractionation between chlorite and water from 170 to 350°C: A preliminary assessment based on partial exchange and fluid/rock experiments: Geochimica et Cosmochimica Acta, v. 63, p. 449–457.

Coleman, M.L., Shepherd, T.J., Durham, J.J., Rouse, J.E., and Moore, G.R., 1982, Reduction of water with zinc for hydrogen isotope analysis: Analytical Chemistry, v. 54, p. 993–995.

Coughlin, T.J., O'Sullivan, P.B., Kohn, B.P., and Holcombe, R.J., 1998, Apatite fission-track thermochronology of the Sierras Pampeanas, central western Argentina: Implications for the mechanism of plateau uplift in the Andes: Geology, v. 26, p. 999–1002.

Dawson, S.E., 1994, The occurrence of gold at the Bajo de la Alumbrera porphyry copper-gold deposit, northwestern Argentina: Unpublished M.Sc. thesis, Tucson, University of Arizona, 135 p.

De Geoffroy, J., and Wignall, T.K., 1972, A statistical study of geological characteristics of porphyry-copper-molybdenum deposits in the Cordilleran belt—application of rating of porphyry prospects: Economic Geology, v. 67, p. 656–668.

de Urreiztieta, M., Gapais, D., Le, C.C., Cobbold, P.R., and Rossello, E., 1996, Cenozoic dextral transpression and basin development at the southern edge of the Puna plateau, northwestern Argentina: Tectonophysics, v. 254, p. 17–39.

Dilles, J.H., Solomon, G.C., Taylor, H.P., Jr., and Einaudi, M.T., 1992, Oxygen and hydrogen isotope characteristics of hydrothermal alteration at the Ann-Mason porphyry copper deposit, Yerington, Nevada: Economic Geology, v. 87, p. 44–63.

Dobson, P.F., Epstein, S., and Stopler, E.M., 1989, Hydrogen isotope fractionation between coexisting vapor and silicate glasses and melts at low pressure: Geochimica et Cosmochimica Acta, v. 53, p. 2723–2730.

Eastoe, C.J., 1978, A fluid inclusion study of the Panguna porphyry copper deposit, Bougainville, Papua New Guinea: Economic Geology, v. 73, p. 721–748.

Faure, K., 2003, $\delta$D values of fluid inclusions water in quartz and calcite ejecta from active geothermal systems: Do values reflect those of original hydrothermal water?: Economic Geology, v. 98, p. 657–660.

Faure, K., Matsuhisa, Y., Metsugi, H., Mizota, C., and Hayashi, S., 2002, The Hishikari Au-Ag epithermal deposit, Japan: Oxygen and hydrogen isotope evidence in determining the source of paleohydrothermal fluids: Economic Geology, v. 97, p. 481–498.

Figueroa, L.A., 1971, Fotolineamientos y mineralización en el norosete Argentino: Primer Simposio Nacional Geología Económica, Buenos Aires, p. 107–124.

Ford, J.H., and Green, D.C., 1977, An oxygen and hydrogen isotope study of the Panguna porphyry copper deposit, Bougainville: Geological Society of Australia Journal, v. 24, p. 63–80.

Giggenbach, W.F., 1992, Isotopic shifts in waters from geothermal and volcanic systems along convergent plate boundaries and their origin: Earth and Planetary Science Letters, v. 113, p. 495–510.

Godeas, M.C., and Segal de Svetliza, S.J., 1980, Alteración hidrotermal y mineralización en el Bajo la Alumbrera, Prov. De Catamarca: Revista Asociación Geología Argentina, v. 35, p. 318–331.

González, O.E., 1975, Geología y alteración en el cobre porfidico "Bajo la Alumbrera:" Rep. Argentina: II. Congreso Ibero-Americano de Geología Económica, 1975, p. 247–270.

Guilbert, J.M., 1995, Geology, alteration, mineralization and genesis of the Bajo de la Alumbrera porphyry copper-gold deposit, Catamarca province, Argentina: Arizona Geological Society Digest, v. 20, p. 646–656.

Gustafson, L.B., and Hunt, J.P., 1975, The porphyry copper deposit at El Salvador, Chile: Economic Geology, v. 70, p. 857–912.

Hall, W.E., Friedman, I., and Nash, J.T., 1974, Fluid inclusion and light stable isotope study of Climax molybdenum deposits, Colorado: Economic Geology, v. 69, p. 884–901.

Halter, W.E, Heinrich, C.A., and Pettke, T, 2004a, Magma evolution and the formation of porphyry Cu–Au ore fluids: Evidence from silicate and sulfide melt inclusions: Mineralium Deposita, v. 389, p. 845–863.

——2004b, Laser-ablation ICP-MS analysis of silicate and sulfide melt inclusions in an andesitic complex II: Evidence for magma mixing and magma chamber evolution: Contributions to Mineralogy and Petrology, v. 147, p. 397–412.

Harris A.C., 2002, The genesis of a porphyry Cu-Au deposit, Farallón Negro Volcanic Complex, NW Argentina: Unpublished Ph.D. thesis, Brisbane, University of Queensland, 281 p.

Harris, A.C., and Golding, S.D., 2002, New evidence of magmatic-fluid related phyllic alteration: Implications for the genesis of porphyry Cu deposits: Geology, v. 30, p. 335–338.

Harris, A.C., Kamenetsky, V.S., White, N.C., van Achterbergh, E., and Ryan, C.G., 2003, Melt inclusions in veins: Linking magmas and porphyry Cu deposits: Science, v. 302, p. 2109–2111.

Harris, A.C., Kamenetsky, V.S., White, N.C., and Steele, D.A., 2004a, Volatile phase separation in silicic magmas at Bajo de la Alumbrera porphyry Cu-Au deposit, NW Argentina: Resource Geology, v. 54, p. 341–356.

Harris, A.C., Allen, C.A., Bryan, S.E., Campbell, I.H., Holcombe, R.J., and Palin, M.J., 2004b, Measuring the longevity of regional volcanism hosting the Bajo de la Alumbrera Cu-Au deposit: Implications for the genesis of porphyry ore deposits: Mineralium Deposita, v. 39, p. 46–67.

Hedenquist, J.W., and Henley, R.W., 1985, The importance of $CO_2$ on freezing point measurements of fluid inclusions: Evidence from active geothermal systems and implications for epithermal ore deposition: Economic Geology, v. 80, p. 1379–1406.

Hedenquist, J.W., and Lowenstern, J.B., 1994, The role of magmas in the formation of hydrothermal ore deposits: Nature, v. 370, p. 519–527.

Hedenquist, J.W., and Richards, J.P., 1998, The influence of geochemical techniques on the development of genetic models for porphyry copper deposits: Reviews in Economic Geology, v. 10, p. 235–256.

Hedenquist, J.W., Arribas, A., and Reynolds, T.J., 1998, Evolution of an intrusion-centered hydrothermal system: Far Southeast Lepanto porphyry and epithermal Cu-Au deposits, Philippines: Economic Geology, v. 93, p. 374–404.

Hemley, J.J., and Hunt, J.P., 1992, Hydrothermal ore-forming processes in the light of studies in rock-buffered systems: II. Some general geologic applications: Economic Geology, v. 87, p. 23–43.

Henley, R.W., and McNabb, A., 1978, Magmatic vapor plumes and groundwater interaction in porphyry copper emplacement: Economic Geology, v. 73, p. 1–20.

Hezarkhani, A., and Williams-Jones, A.E., 1998, Controls of alteration and mineralization in the Sungun porphyry copper deposit, Iran: Evidence from fluid inclusions and stable isotopes: Economic Geology, v. 93, p. 651–670.

Horita, J., Cole, D.R., and Wesolowski, D.J., 1995, The activity-composition relationship of oxygen and hydrogen isotopes in aqueous salt solutions: III. Vapor-liquid water equilibration of NaCl solution to 350°C: Geochimica et Cosmochimica Acta, v. 59, p. 1139–1151.

Jordan, T.E., and Allmendinger, R.W., 1986, The Sierras Pampeanas of Argentina: A modern analogue of Rocky Mountain foreland deformation: American Journal of Science, v. 286, p. 737–764.

Kleinert, K., and Strecker, M.R., 2001, Climate change in response to orographic barrier uplift: Paleosol and stable isotope evidence from the late Neogene Santa Maria basin, northwestern Argentina: Geological Society of America Bulletin, v. 113, p. 728–742.

Llambías, E.J., 1972, Estructura del grupo volcanico Farallón Negro, Catamarca, República Argentina: Revista de la Asociation Geologica Argentina, v. 27, p. 161–169.

Lowell, J.D., and Guilbert, J.M., 1970, Lateral and vertical alteration-mineralization zoning in porphyry ore deposits: Economic Geology, v. 65, p. 373–408.

Marumo, K., Nagasawa, K., and Kuroda, Y., 1980, Mineralogy and hydrogen isotope geochemistry of clay minerals in the Ohnuma geothermal area, northeastern Japan: Earth and Planetary Science Letters, v. 47, p. 255–262.

Matsuhisa, Y., Goldsmith, J.R., and Clayton, R.N., 1979, Oxygen isotope fractionation in the system quartz-albite-anorthite-water: Geochimica et Cosmochimica Acta, v. 43, p. 1131–1140.

Matthews, A., Goldsmith, J.R., and Clayton, R.N., 1983, Oxygen isotope fractionations involving pyroxenes: The calibration of mineral-pair geothermometers: Geochimica et Cosmochimica Acta, v. 47, p. 631–644.

Meinert, L.D., Hedenquist, J.W., Satohi, H., and Matsuhisa, Y., 2003, Formation of anhydrous and hydrous skarn in Cu-Au ore deposits by magmatic fluids: Economic Geology, v. 98, p. 147–156.

Méndez, V., 1997, Yacimiento Bajo la Alumbrera, Provincia de Catamarca, República Argentina: Revista de la Asociación Argentina de Geólogos Economistas, v. 11, p. 15–30.

Meyer, C., and Hemley, J.J., 1967, Wall rock alteration, *in* Barnes, H.L., ed., Geochemistry of hydrothermal ore deposits: New York, Toronto, and London, International, Holt, Rinehart and Winston, p. 166–235.

Moore, W.J., and Nash, J.T., 1974, Alteration and fluid inclusion studies of the porphyry copper ore body at Bingham, Utah: Economic Geology, v. 69, p. 631–645.

O'Neil, J.R., and Taylor, H.P., 1969, Oxygen isotope equilibrium between muscovite and water: Journal of Geophysical Research, v. 74, p. 1414–1437.

Pallister, J.S., Hoblitt, R.P., Meeker, G.P., Knight, R.J., and Siems, D.F., 1996, Magma mixing at Mount Pinatubo: Petrographic and chemical evidence from the 1991 deposits, *in* Newhall Christopher, G., and Punongbayan Raymundo, S., eds., Fire and mud: Eruptions and lahars of Mount Pinatubo, Philippines: Quezon City, Philippines; University of Washington Press United States, p. 687–731.

Pardo-Casas, F., and Molnar, P., 1987, Relative motion of the Nazca (Farallón) and South American plates since Late Cretaceous time: Tectonics, v. 6, p. 233–248.

Pollard, P.J., Andrew, A.S., and Taylor, R.G., 1991, Fluid inclusion and stable isotope evidence for the interaction between granites and magmatic hydrothermal fluids during the formation of disseminated and pipe-style mineralization at the Zaalplaats tin mine: Economic Geology, v. 86, p. 121–141.

Proffett, J.M., 2003, Geology of the Bajo de la Alumbrera porphyry copper-gold deposit, Argentina: Economic Geology, v. 98, p. 1535–1574.

Reyes, A.G., 1990, Petrology of Philippine geothermal systems and the application of alteration mineralogy to their assessment: Journal of Volcanology and Geothermal Research, v. 43, p. 279–309.

Reynolds, J.H., Tabbutt, K.T., Johnson, N.M., and Jordan, T.E., 1987, Nonsystematic uplift of the northwestern Sierras Pampeanas, Catamarca Province, Argentina: Interpretation of magnetic polarity stratigraphy data [abs.]: Geological Society of America Abstracts with Programs, v. 19, p. 817.

Reynolds, T.J., and Beane, R.E., 1985, Evolution of hydrothermal characteristics at the Santa Rita, New Mexico, porphyry copper deposit: ECONOMIC GEOLOGY, v. 80, p. 1328–1347.

Roedder, E., 1971, Fluid inclusion studies on the porphyry-type ore deposits at Bingham, Utah, Butte, Montana, and Climax, Colorado: ECONOMIC GEOLOGY, v. 66, p. 98–118.

Sasso, A.M., 1997, Geological evolution and metallogenetic relationships of the Farallón Negro Volcanic Complex, NW Argentina: Unpublished Ph.D. thesis, Kingston, Canada, Queens University, 842 p.

Sasso, A.M., and Clark, A.H., 1998, The Farallón Negro Group, northwest Argentina: Magmatic, hydrothermal and tectonic evolution and implications for Cu-Au metallogeny in the Andean back arc: Society of Economic Geologists Newsletter, no. 34, p. 1, 8–18.

Selby, D., Nesbitt, B.E., Creaser, R.A., Reynolds, P.H., and Muehlenbachs, K., 2001, Evidence for a nonmagmatic component in potassic hydrothermal fluids of porphyry Cu-Au-Mo systems, Yukon, Canada: Geochimica et Cosmochimica Acta, v. 65, p. 571–587.

Sheets, R.W., Nesbitt, B.E., and Muehlenbachs, K., 1996, Meteoric water component in magmatic fluids from porphyry copper mineralization, Babine Lake area, British Columbia: Geology, v. 24, p. 1091–1094.

Sheppard, S.M.F., and Gilg, H.A., 1996, Stable isotope geochemistry of clay minerals: Clay Minerals, v. 31, p. 1–24.

Sheppard, S.M.F., and Gustafson, L.B., 1976, Oxygen and hydrogen isotopes in the porphyry copper deposit at El Salvador, Chile: ECONOMIC GEOLOGY, v. 71, p. 1549–1559.

Sheppard, S.M.F., and Taylor, H.P., 1974, Hydrogen and oxygen isotope evidence for the origins of water in the Boulder batholith and the Butte ore deposits: ECONOMIC GEOLOGY, v. 64, p. 755–777.

Sheppard, S.M.F., Nielsen, R.L., and Taylor, H.P., 1969, Oxygen and hydrogen isotope ratios of clay minerals from porphyry copper deposits: ECONOMIC GEOLOGY, v. 64, p. 755–777.

——1971, Hydrogen and oxygen isotope ratios in minerals from porphyry copper deposits: ECONOMIC GEOLOGY, v. 66, p. 515–542.

Shmulovich, K.I., Landwehr, D., Simon, K., and Heinrich, W., 1999, Stable isotope fractionation between liquid and vapor in water-salt systems up to 600°C: Chemical Geology, v. 157, p. 343–354.

Sillitoe, R.H., 1973, The tops and bottoms of porphyry copper deposits: ECONOMIC GEOLOGY, v. 68, p. 799–815.

——2000, Gold-rich porphyry deposits: descriptive and genetic models and their role in exploration and discovery: Reviews in Economic Geology, v. 13, p. 315–345.

Sillitoe, R.H., and Gappe, I.M., Jr., 1984, Philippine porphyry copper deposits: Geologic setting and characteristics: Bangkok, Thailand, United Nations ESCAP, CCOP Technical Publication 14, 89 p.

Strecker, M.R., Cerveny, P., Bloom, A.L., and Malizia, D., 1989, Late Cenozoic tectonism and landscape development in the foreland of the Andes: Northern Sierras Pampeanas (26°– 28° S), Argentina: Tectonics, v. 8, p. 517–534.

Stults, A., 1985, Geology of the Bajo de la Alumbrera porphyry copper and gold prospect, Catamarca province, Argentina: Unpublished M.Sc. thesis, Tucson, University of Arizona, 75 p.

Suzuki, T., and Epstein, S., 1976, Hydrogen isotope fractionation between OH-bearing minerals and water: Geochimica et Cosmochimica Acta, v. 40, p. 1229–1240.

Sverjensky, D.A., Hemley, J.J., and D'Angelo, W.M., 1991, Thermodynamic assessment of hydrothermal alkali feldspar-mica-aluminosilicate equilibria: Geochimica et Cosmochimica Acta, v. 55, p. 989–1004.

Tabbutt, K.D., 1990, Temporal constraints on the tectonic evolution of Sierra de Famatina, northwestern Argentina, using the fission-track method to date tuffs interbedded in synorogenic clastic sedimentary strata: Journal of Geology, v. 98, p. 557–566.

Taylor, B.E., 1986, Magmatic volatiles: Isotopic variation of C, H, and S: Reviews in Mineralogy, v. 16, p. 185–225.

——1992, Degassing of $H_2O$ from rhyolite magma during eruption and shallow intrusion, and the isotopic composition of magmatic water in hydrothermal systems: Geological Survey of Japan Memoir 279, p. 190–195.

Taylor, B.E., Eichelberger, J.C., and Westrich, H.R., 1983, Hydrogen isotopic evidence of rhyolitic magma degassing during shallow intrusion and eruption: Nature, v. 306, p. 541–545.

Taylor, B.E., Ford, E.E., and Friedrichsen, H., 1979, Stable isotope and fluid inclusion studies of GEM-bearing granitic pegmatite-aplite dikes, San Diego Co., California: Contributions to Mineralogy and Petrology, v. 68, p. 187–205.

Taylor, H.P., 1974, The application of oxygen and hydrothermal isotope studies to problems of hydrothermal alteration and ore deposition: ECONOMIC GEOLOGY, v. 69, p. 843–883.

Ulrich, T., 1999, Genesis of the Bajo de la Alumbrera porphyry Cu-Au deposit, Argentina: Geological, fluid geochemical and isotopic implications: Unpublished Ph.D. thesis, Zürich, Swiss Fedral Institute of Technology, 207 p.

Ulrich, T., and Heinrich, C.A., 2002, Geology and alteration geochemistry of the porphyry Cu-Au deposit at Bajo de la Alumbrera, Argentina: ECONOMIC GEOLOGY, v. 97, p. 1865–1888.

Ulrich, T., Günthur, D., and Heinrich, C.A., 2002, The evolution of a porphyry Cu-Au deposit, based on LA-ICP-MS analysis of fluid inclusions: Bajo de la Alumbrera, Argentina: ECONOMIC GEOLOGY, v. 97, p. 1889–1920.

Watanabe, Y., and Hedenquist, J.W., 2001, Mineralogic and stable isotope zonation at the surface over the El Salvador porphyry copper deposit, Chile: ECONOMIC GEOLOGY, v. 96, p. 1775–1798.

Zaluski, G., Nesbitt, B., and Muehlenbachs, K., 1994, Hydrothermal alteration and stable isotope systematics of the Babine porphyry Cu deposits, British Columbia: Implications for fluid evolution of porphyry systems: ECONOMIC GEOLOGY, v. 89, p. 1518–1541.

Zhang L.G., Liu J.X., Zhou H.B., and Chen Z.S., 1989, Oxygen isotope fractionation in the quartz-water-salt system: ECONOMIC GEOLOGY, v. 89, p. 1643–1650.

## APPENDIX

### Sample Locations

*Potassic alteration assemblages*

ACH0125 (GR. –66°36'30.708, –27°19'41.88):

P2 (?) Porphyry altered by K-feldspar-biotite-magnetite-quartz. Intense pervasive biotite-magnetite alteration obscures phenocrysts and groundmass mineralogy. Biotite phenocrysts are recrystallized and the groundmass feldspars are altered to a mosaic of biotite-quartz-K-feldspar ± chlorite-rutile-apatite. Quartz ± chalcopyrite-K-feldspar veins cut this pervasive alteration. The $\delta^{18}O$ and $\delta D$ values of quartz were determined for these veins. Chlorite ± illite alteration affects the biotite phenocrysts and less commonly the secondary biotite.

ACH99105 (DDH49.2-46.3, 143m):

Intensely altered porphyritic rock (P2 or Los Amarillos Porphyry?). The groundmass is altered by K-feldspar and lesser illite and chlorite. Quartz-chlorite ± anhydrite-chalcopyrite veins cut the pervasive alteration assemblage. K-feldspar occurs in the vein selvage but has been replaced in part by illite (?). Handpicked quartz was used for isotopic anaylsis. Polyphase brine (±opaque phases including hematite) and vapor-rich (with a single opaque phase) fluid inclusions were studied from this quartz vein.

ACH9984 (DDH49-50.1, 75m):

Early P3 Porphyry altered by K-feldspar-biotite ± quartz-magnetite. Intense pervasive K-feldspar-biotite-quartz ± chalcopyrite-magnetite has obliterated the groundmass. Diffuse quartz-chalcopyrite veins cut this potassic alteration assemblage. Plagioclase phenocrysts are altered by illite ± chlorite. Patches of the groundmass also are altered by chlorite. Rare pyrite veins cut all alteration stages. Biotite from the pervasive alteration was drilled out for stable isotope analysis.

ACH9985 (DDH50.46.43, 613.2m):

Early P3 Porphyry altered by K-feldspar-biotite. Plagioclase phenocrysts are largely replaced by K-feldspar. Irregular patches of ragged biotite have replaced the groundmass. Biotite from this pervasive alteration was separated for stable isotope analysis.

ACH9983 (DDH49-64.3, 754m):

Early P3 Porphyry altered by magnetite-quartz-chalcopyrite. Pervasive K-feldspar (±biotite) and magnetite alters the groundmass. Biotite is altered to chlorite. Plagioclase (?) phenocrysts are replaced by illite (±chlorite). Quartz from a single magnetite-quartz-chalcopyrite vein (inferred as part of K-feldspar alteration) was used for isotopic analysis. Fluid inclusion trails occurring in the magnetite-quartz-chalcopyrite vein were studied. Isotope analyses were also undertaken on drilled illite separates from the altered feldspars.

ACH9973 (DDH48.4-54, 139m):

Biotite altered Early P3 Porphyry. Primary igneous texture is largely obliterated. Hornblende and/or biotite (?) have been replaced by biotite and chlorite. Bladed muscovite occurs throughout the sample. Quartz-K-feldspar and quartz-magnetite-biotite veins cut the porphyry. Stringers of chlorite-illite also cut the sample. Quartz separated from quartz-magnetite-biotite veins was used for stable isotope analysis.

ACH9999 (DDH51-56, 52m):

Intense, pervasively biotite-magnetite altered P2 Porphyry. The groundmass has been largely replaced by biotite-magnetite, whereas the feldspar phenocrysts are replaced by K-feldspar. Stringers of quartz-magnetite cut the porphyry. Handpicked quartz was used for stable isotope analysis. Phenocrystic and hydrothermal biotite has been largely replaced by chlorite ± illite. Secondary inclusion trails of liquid-rich and vapor inclusions were studied from igneous quartz. Coexisting simple brine inclusions and rare vapor inclusions occurring in a late quartz vein (with a distinct illite-rich alteration selvage) also were characterized.

ACH99153 (DDH49.2-46.3, 446m):

Biotite ± K-feldspar-quartz altered Early P3 Porphyry. Biotite-magnetite replaces the groundmass. Quartz-magnetite ± biotite veins cut the porphyry. Quartz from these veins was used for isotopic anaylsis.

ACH99157 (DDH47-64.3, 794m):

Biotite-K-feldspar altered Late P3 Porphyry (?). Plagioclase phenocrysts are largely replaced by K-feldspar. K-feldspar-biotite and magnetite replace the groundmass. Quartz-magnetite veins cut the porphyry. This sample is from the "barren core" of the deposit. The $\delta^{18}O$ and $\delta D$ values of quartz were determined for these veins.

ACH9995 (49.2-46.3, 263m):

Los Amarillos Porphyry altered by K-feldspar ± magnetite-biotite-chalcopyrite and illite-pyrite assemblages. Sample cut by quartz-chalcopyrite ± magnetite and pyrite-quartz veins. Microthermometric experiments were undertaken on primary (brine and vapor) inclusions in the quartz-chalcopyrite veins. Liquid-rich and vapor inclusions inferred to be associated with development of the illite-rich alteration assemblage were studied from secondary fluid inclusion trails cutting igneous quartz.

*Propylitic alteration assemblages*

BAL00/263 (GR. –66°36'36.648, –27°19'24.456):

Chlorite (±hematite) has replaced the groundmass feldspars in this volcaniclastic rock. This chlorite was used for stable isotope analysis.

*Intermediate argillic alteration assemblages*

ACH9987 (DDH49-64.3, 690m):

K-feldspar-biotite altered Early P3 Porphyry cut by magnetite-chalcopyrite-quartz vein with distinct chlorite-rich selvages. Biotite near the vein has been completely replaced by

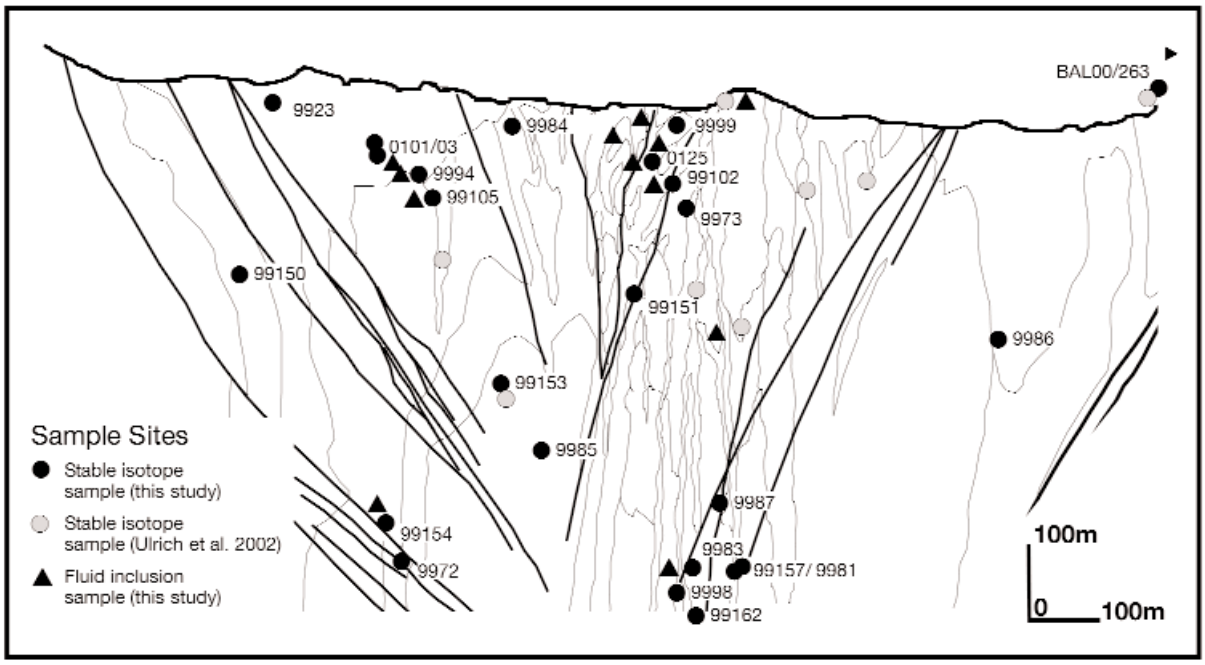


FIG. A1. Location of samples on which stable isotope analyses were conducted, displayed in section A-A', showing the distribution of hydrothermal alteration assemblages (Bajo de la Alumbrera, section 49N; Proffett, 2003).

chlorite. Away from the vein, biotite is unaffected. Both biotite and chlorite separates from this sample were used for stable isotope analysis.

*Phyllic alteration assemblages*

ACH9923 (GR. –66°36'43.740, –27°19'53.040):

K-feldspar-quartz ± magnetite altered P2 Porphyry cut by quartz ± chalcopyrite ± magnetite veinlets. Clots of chlorite-illite ± quartz have replaced the groundmass. Chalcopyrite-pyrite veins (with chlorite-illite alteration selvage) cut the porphyry. Illite-pyrite-chalcopyrite veins cut all early alteration assemblages. The illite-rich veins were used for stable isotope analysis.

ACH9994 (DDH49.2-46.3, 106.0m):

Texturally destructive illite ± quartz-pyrite-chlorite assemblage in Los Amarillos (?) Porphyry. Plagioclase (?) phenocrysts are commonly replaced by illite. Pyrite (and lesser chalcopyrite) is disseminated throughout but is particularly concentrated in chlorite-illite clots. Quartz-magnetite stringers occur throughout the sample. Pyrite veins cut earlier quartz-pyrite veins, whereas anhydrite veins cut all earlier vein stages. A selvage of illite (?) occurs along the edge of the quartz-pyrite veins. Handpicked quartz was used for oxygen isotope analysis. Distinct secondary inclusion trails comprising liquid-rich (<20 vol % liquid) aqueous and vapor-rich (<20 vol % vapor) inclusions were studied from the quartz-pyrite veins.

ACH99162 (DDH47-64.3, 849.6m):

Late P3 (?) Porphyry intensely altered by K-feldspar alteration that has been overprinted by feldspar destructive alteration assemblages. Secondary biotite also occurs as irregular clots that replace the groundmass. Biotite is replaced by chlorite. Magnetite-quartz stringers also occur throughout the sample. All feldspars are replaced by illite (±chlorite). The most illite-rich parts of the sample were used for stable isotope analysis.

ACH9986 (DDH47-64.3, 264.5m):

Undifferentiated plagioclase-phyric volcanic rock. Both phenocrysts and groundmass have been largely replaced by illite. Quartz-pyrite veins cut this pervasive alteration assemblage. Illite was used for oxygen and hydrogen isotope analysis.

ACH99150 (DDH49.2-46.3, 262.0m):

Intensely altered fine-grained plagioclase-phyric (undifferentiated) volcanic rock. The groundmass is largely replaced by chlorite-illite ± quartz. The occurrence of magnetite clots implies that this alteration overprinted pervasive biotite. Magnetite-chalcopyrite and quartz-anhydrite veins cut the potassic alteration assemblages. In part, the groundmass of the sample is entirely replaced by illite and pyrite. Separates from these patches were used for stable isotope analysis.

ACH9994 (DDH49.2-46.3, 106.0m):

Los Amarillos Porphyry altered by K-feldspar ± biotite ± quartz and illite-pyrite-quartz ± chlorite assemblages. Feldspars and patches of the groundmass are replaced by illite ± pyrite. Pyrite ± quartz veins cut quartz ± magnetite veins. Illite-rich zones have been used for isotopic anaylsis.

ACH0101 (DDH51-45.2; 107.0m):

Los Amarillos Porphyry altered by K-feldspar ± biotite ± quartz. Irregular patches of biotite occur throughout the

groundmass. K-feldspar-magnetite ± quartz and magnetite-quartz veins cut the porphyry. Illite-pyrite-quartz ± chlorite assemblages have overprinted all potassic alteration assemblages. Feldspars and patches of the groundmass are replaced by illite ± pyrite. Quartz-pyrite veins also occur. Illite-rich zones were used for stable isotope analysis. Microthermometry was conducted on secondary liquid (<20 vol % vapor) aqueous inclusions in the quartz-pyrite veins.

ACH0103 (DDH51-45.2, 121m):

Biotite and illite altered feldspar-phyric (undifferentiated volcanic) rock. The primary igneous texture of the rock has been obliterated. The groundmass has been replaced by biotite ± K-feldspar-magnetite and then overprinted by illite-chlorite-pyrite assemblages. All phenocrysts are replaced by illite-pyrite. Quartz-magnetite, anhydrite, quartz-illite-pyrite and pyrite (±illite-chlorite) veins cut the rock. Illite-rich zones were used for stable isotope analysis. Secondary liquid-rich (up to 10 vol % vapor) aqueous inclusions (occurring in quartz phenocrysts) parallel to single pyrite (±illite-chlorite) vein were studied. Similar secondary inclusion trails also were observed cutting earlier quartz-magnetite veins and appear related to fracture-controlled illite-chlorite alteration.

ACH99102 (DDH48.4-54, 124.4m):

Early P3 Porphyry with relatively fresh magmatic biotite and plagioclase phenocrysts. The groundmass and some plagioclase phenocrysts have been altered by biotite. Veins (similar to A veins) consist of quartz, with lesser amounts of K-feldspar ± hornblende-biotite-magnetite-chalcopyrite and pyrite. Veinlets of magnetite and a distinct (up to 0.5 mm wide) chlorite-illite-pyrite vein also occur in this sample. The most illite rich alteration selvages were drilled for stable isotope analysis. Polyphase brine inclusions found in quartz veins (P vein and/or A vein) were studied. Microthermometry also was conducted on simple brine inclusions coexisting with rare vapor-rich inclusions in trails within a quartz vein associated with the development of the pervasive illite (?) alteration assemblages. Secondary inclusion trails (characterized by simple brine and vapor-rich inclusions) cutting igneous quartz were also studied. These secondary inclusion trails parallel a chlorite-illite-pyrite vein.

ACH99151 (DDH49-50.1, 315.8m):

Biotite altered Late P3 Porphyry. The groundmass has been partly replaced by biotite, which is overprinted by more pervasive chlorite alteration. Thin veinlets of quartz-magnetite cut the rock. Chlorite ± illite replaces plagioclase. Biotite is altered to chlorite. Diffuse zones of intense fracture-controlled illite ± chlorite-quartz alteration also cut the rock. This alteration is characterized by near-total replacement of feldspar phenocrysts and partial replacement of the groundmass by illite and chlorite. The most intense illite rich zones were used for stable isotope analysis.

ACH99154 (DDH49.1-40, 710.0m):

Undifferentiated andesitic volcanic (or volcaniclastic?) rock altered by texturally destructive and pervasive illite-rich alteration assemblages. This alteration zone occurs immediately adjacent to a zone (15 m) of sphalerite- and galena-bearing carbonate-quartz veins. The most intense illite rich zones were used for stable isotope analysis.

*Porphyritic intrusions (phenocrysts)*

ACH9981 (DDH47-64.3, 786.5m):

Relatively fresh Late P3 Porphyry, with large (up to 8 mm) biotite phenocrysts. Although rarely seen, this biotite is locally replaced by chlorite. Associated with the chloritized biotite are veinlets of pyrite. Both $\delta^{18}O$ and $\delta D$ values have been determined for the freshest biotite phenocrysts in this sample.

ACH9998 (DDH49-64.3, 770.9m):

A phase of the Late P3 Porphyry (?). Biotite and alkali feldspar phenocrysts are anhedral, subhedral, and euhedral. The aphanitic groundmass comprises quartz and feldspar. Small anhedral to subhedral apatite and zircon crystals are dispersed through the groundmass. The sample lacks pervasive alteration but is cut by rare magnetite veins.

ACH9972 (DDH49-64.3, 771.0m):

Relatively unaltered Late P3 Porphyry (?) phase (as sample ACH9998), with fresh plagioclase, alkali feldspar, and biotite phenocrysts. Biotite phenocrysts are up to 8 mm.